Title: Role of Atomic Structure Calculations: From Fundamental Physics to Technological Advancements

Speakers: Bindiya Arora

Collection/Series: Colloquium

Subject: Other

Date: December 11, 2024 - 2:00 PM

URL: https://pirsa.org/24120030

Abstract:

Atomic structure calculations are critical for advancing fundamental physics and driving technological innovation. They provide essential data for experimental design and interpretation, especially when direct measurements are challenging. These calculations are pivotal in areas such as quantum computing, atomic clocks, quantum sensors, and cold atom physics, as well as in fundamental research, including parity non-conservation, dark matter searches, and gravitational wave detection.

This presentation will explore how precise atomic property calculations propel both technological advancements and our understanding of nature. I will discuss:

Our research group's contributions to high-precision atomic property calculations for technological developments in cold atom physics, atomic clocks, and other applications.

Recent work addressing challenges in atomic structure theory, including basis sets, spurious states, and modeling properties of Rydberg atoms for quantum computing.

The design and underlying concepts of the atomic cyberinfrastructure under development in our group.

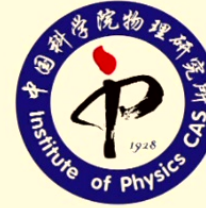# Role of Atomic Structure Calculations
From Fundamental Physics to Technological Advancement
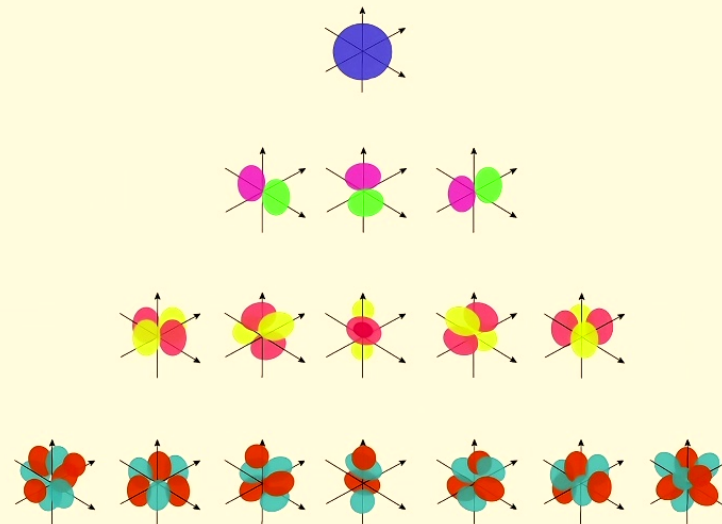
Bindiya Arora
Perimeter Institute for Theoretical Physics, Canada
University of Waterloo, Canada
Guru Nanak Dev University, India

(2011-2022)

ATOMS@GNDU

PhD. Scholars (8)

Jasmeet Kaur (2018) (Baba Fareed University)

Sukhjit Singh (2018) (Dept. of Education, Punjab)

Kiranpreet Kaur (2018)

Maninder Kaur (2019) (DAV College)

Mandeep Kaur (2021) (Chandigarh University)

Jyoti (2023) (Peking University)

Harpreet Kaur (2023) (Khalsa College)

Vipul Badhan (IVGS, UWaterloo & PI)

Masters Students (34)

Shankar Dutt(Australian National University)

Paras Dev (Paris Saclay, France)

Preeti Sharma (IITD, India)

Sumeet Kaur (Friedrich-Alexander University Erlangen, Germany)

Rishabh Nakra (SecretsOfTheUniverse)

Danish Furekh (GSI Helmoltz Institute, Germany)

Sheffali (U Manitoba)

Simranpreet (Institute of Space Sciences, Barcelona)

Tavshabd(University of Queensland)
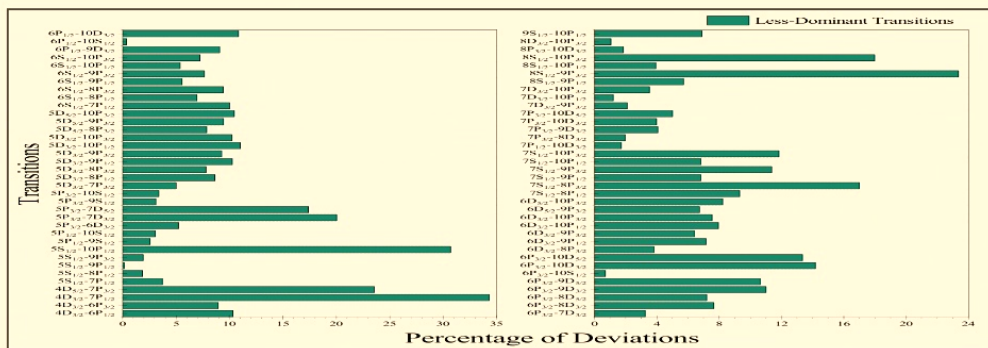
Funding (5)

DST FAST Track

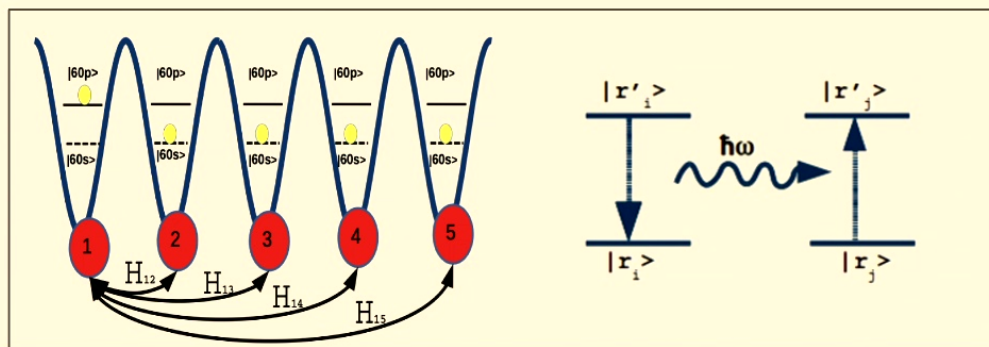UGC Start-up

CSIR

DST-SERB

SERB TARE

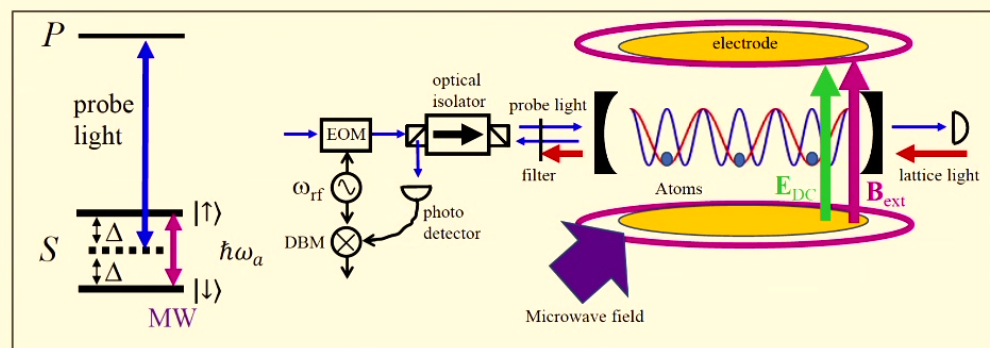# Atoms@GNDU

Spectroscopic data

Less-Dominant Transitions

J. Phys. B Vol 53, 6 (2020), Phy. Rev. A Vol 102, 041101(R) (2020), ADNDT, 21 (2020), V. 137 101381, Atoms 2022, 10(3), 72 (2020), ADNDT 140, 101422 (2021), MNRAS ,Vol 507, 3, Pages 4030–4043, MNRAS, Vol 511, 2, (2022)

Quantum Sensors

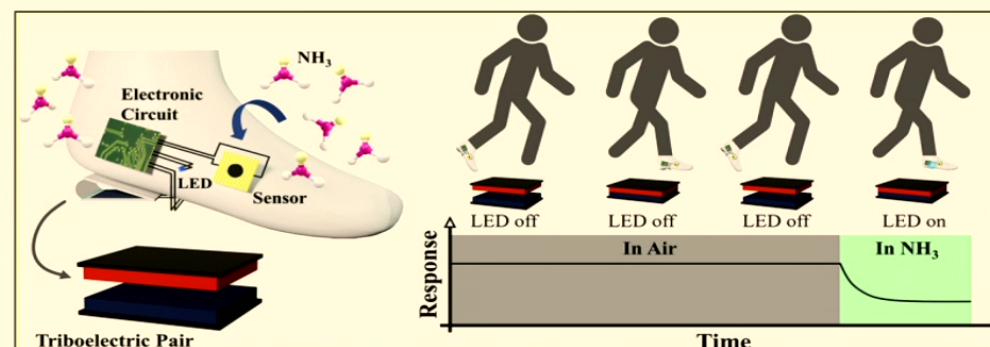Quantum Sci.Technol. 4, 044008 (2021), Phys. Scr. 98 105106 (2023)

Rydberg Atoms & Quantum Computation

Eur. Phys. J. D (2018) 72: 150, Phys. Scr. 98 105106 (2023)

Gas sensors

J. Phys. B. 47(2014) 155002, Phys. Rev. B 90, 245405 (2014), Phys. Rev. A 92, 032704 (2015), Phys. Lett. A 380, 3366 (2016), J Mater Sci: Mater Electron (2017), Phys. Rev. A 102, 022817 (2020), Phys. Rev. A 104, 012806 (2021), ACS Sensors 7, 1, 312–321 (2022)

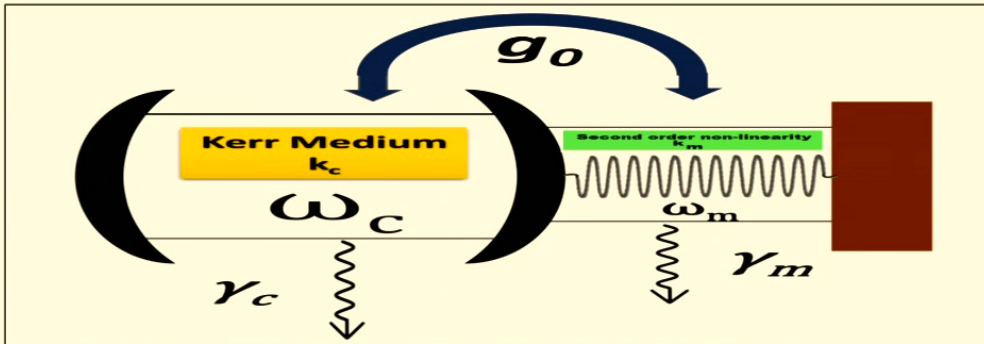**Jasmeet Kaur**   Sukhjit Singh   Kiranpreet Kaur   **Maninder Kaur**   **Mandeep Kaur**   **Harpreet Kaur**   Jyoti Arora   Vipul Badhan
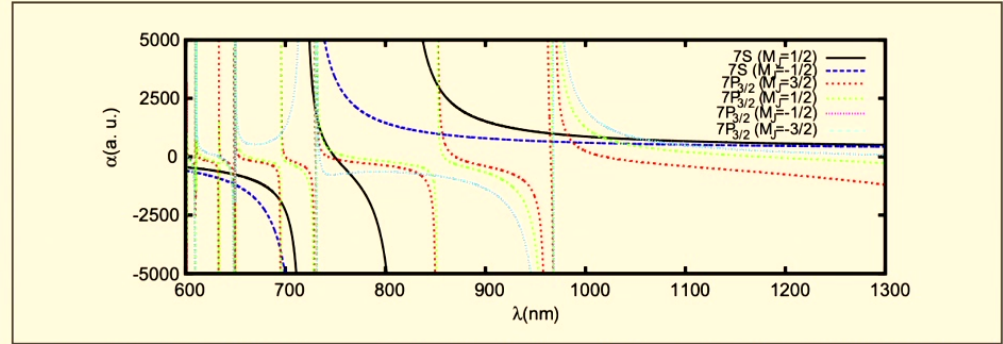
Atoms@GNDU

## Quantum revivals & collapses

Parmana Vol XX, No. X, pages 1-18 (2015), Eur. Phys. J. D (2018) 72: 136, Atoms 2022, *10*(3), 81

Cold Atom Traps

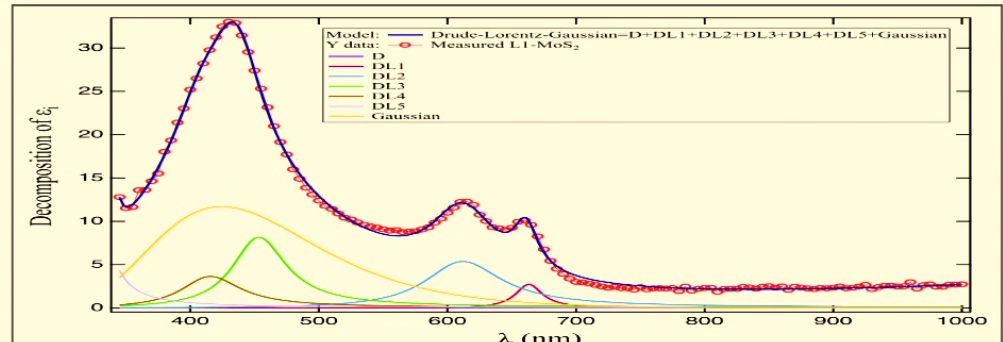Phys. Rev. A 93, 063422 (2016), Phys. Rev. A 94,J. Phys. B, Volume 49, Number 14 (2016) 023418 (2016)J. Phys. B, Volume 49, Number 14 (2016), Phys. Rev. A 95, 042501 (2017), Phys. Rev. A 93, 063422 (2016), Phys. Rev. A **94**, 023418 (2016), Phys. Rev. A 95, 042501 (2017), Atoms 8, 79 (2020), Phys. Rev. A **105**, 032819 (2022), Atoms 2022, *10*(3) (2022)

Atomic Clocks
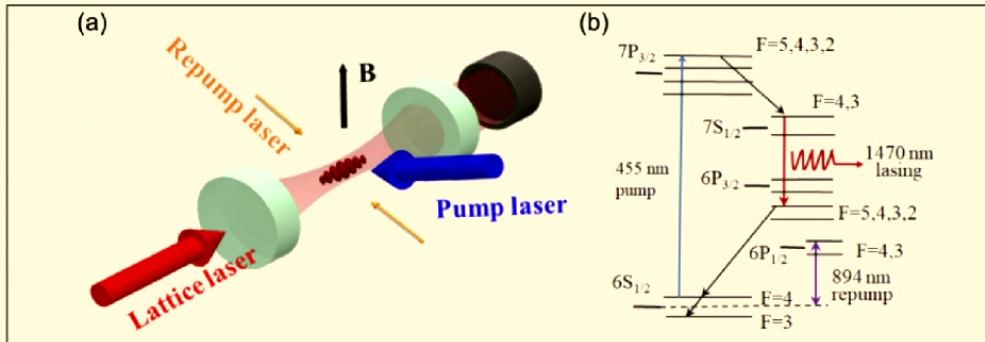
Phys. Rev. A 102, 041101(R) (2020), Atoms 2022, 10(3), 72 (2022), J. Phys. B, 50, 20 (2017), Phys. Rev. A 98, 013406(2018), Phys. Rev. A **102**, 041101(R) (2020), Eur. Phys. J. D (2022) **76**: 252, Phys. Rev. A **108** (2023)

Dispersion interactions

Phys. Rev. A 93, 063422 (2016), Phys. Rev. A 94, 023418 (2016), J. Phys. B, Vol 49, 14 (2016), Phys. Rev. A 95, 042501 (2017), Phys. Rev. A 91, 012705 (2015), Phys. Rev. A 89, 022511(2014), Phys. Rev. A 106, 04281(2022), Physica Scripta Vol 95, 9 (2020), Physica Scripta B 624, 413422 (2021)

Jasmeet Kaur   Sukhjit Singh   Kiranpreet Kaur   Maninder Kaur   Mandeep Kaur   Harpreet Kaur   Jyoti Arora   Vipul Badhan

RESEARCH WORK

1 High precision atomic structure calculations
Portal for atomic data

2 Optical trapping
Magic & tune out wavelengths

3 Atomic clocks
New proposals, Systematics shifts

4 Dispersion interaction
Atom-atom, atom-surface

5 Role of basis
Basis-set war, spurious states

6 Future directions
Atomic Physics Package

ATOMIC STRUCTURE CALCULATIONS

High-precision atomic structure calculations play a vital role in several applications and in investigating fundamental physics

Solve Equation for Hamiltonian → Get Precise Wavefunctions → Calculate Properties → Probe New Physics

Properties

- Energies
- Electric Dipole Moments
- Dipole and Quadrupole Polarizabilities
- Lifetimes and Oscillator Strength
- Systematic shifts
- Magic and tune-out wavelengths
- Rydberg Properties

Applications

- Precise frequency standards
- Variation of Fundamental Constants
- Dark Matter Searches
- Quantum Computation
- Stability of Bose-Einstein Condensates
- Subtle signatures like Parity Violation
- Astrophysics, etc.

SOLVING EQUATIONS

Solving the Schrodinger or Dirac equation have always been a center
of interest for physicists and chemists around the globe

Solving these
Equations Exactly → Not Always
Possible → Achieve Close to
Exact if Not Exact

Helium Atom Ground-State Energy

Methods	Energy/E_h	% Error
Neglecting Interelectronic Repulsion	- 4.0000	37.77
First-order Perturbation Theory	- 2.7500	5.28
Second-order Perturbation Theory	- 2.9077	0.15
Thirteenth-order Perturbation Theory	- 2.90372433	0.01
Hartree-Fock	- 2.86168	1.43
Experimental value	*- 2.9033*	-

METHODS

Challenge is to solve for the repulsion term in Hamiltonian. Perturbative and variational methods are used to handle the repulsion term but these methods are not feasible for atoms having large number of electrons

Many Body Hamiltonian

$$H(\vec{r}_1, \vec{r}_2, \cdots, \vec{r}_N) = \sum_{i=1}^{N} h_0(\vec{r}_i) + \frac{1}{2}\sum_{i \neq j}^{N} \frac{1}{|\vec{r}_{ij}|}$$

One Electron Dirac Hamiltonian

$$h_0(\vec{r}) = c\,\alpha \cdot p + \beta c^2 + V_{nuc}(\vec{r})$$

Dirac Hartree Fock method can solve for this hamiltonian with much lesser computational efforts

Dirac Hartree Fock

- Independent Particle Approximation
- Central Field Model
- Variational Method
- Self Consistent
- Works for Heavier Atoms

Post Hartree Fock

- Many Body Perturbation Theory
- Configuration Interaction
- Coupled Cluster
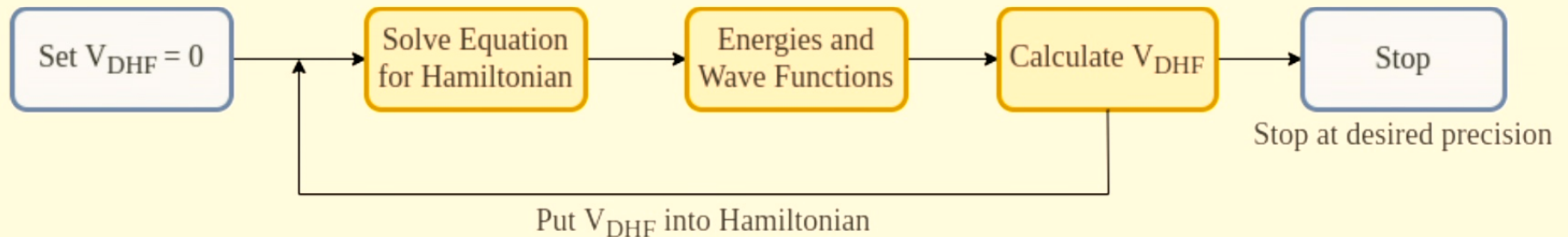
DIRAC HARTREE FOCK

Electrons are assumed to move independently of each other in an average field due to the nucleus and the other electrons

Key Points

- Most successful method for many body calculation
- It self consistently obtain correct wavefunctions
- Being variational method it always gives energies at upper bound

Central Field Model and Self Consistency

- The average potential on an electron due to nucleus and all other electron is considered to be spherically symmetric.
- This potential is called as Dirac Hartree Fock potential and is used to solve equations self consistently.

$$\text{Set } V_{DHF} = 0 \rightarrow \text{Solve Equation for Hamiltonian} \rightarrow \text{Energies and Wave Functions} \rightarrow \text{Calculate } V_{DHF} \rightarrow \text{Stop}$$

Stop at desired precision

Put V_{DHF} into Hamiltonian

DIRAC HARTREE FOCK

Electrons are assumed to move independently of each other in an average field due to the nucleus and the other electrons

DHF Potential $\quad V_{\text{DHF}}|\phi_a(\vec{r}_1)\rangle = V_{\text{Dir}}|\phi_a(r)\rangle + V_{\text{Exc}}|\phi_a(r)\rangle$

Independent Particle Approximation

Complete wave function is represented by Slater determinant of independent orbitals as

$$\psi(\vec{r}_1, \vec{r}_2, \cdots, \vec{r}_N) = \frac{1}{\sqrt{N!}} \begin{vmatrix} \phi_1(\vec{r}_1) & \phi_2(\vec{r}_1) & \cdots & \phi_N(\vec{r}_1) \\ \phi_1(\vec{r}_2) & \phi_2(\vec{r}_2) & \cdots & \phi_N(\vec{r}_2) \\ \vdots & \vdots & \ddots & \vdots \\ \phi_1(\vec{r}_N) & \phi_2(\vec{r}_N) & \cdots & \phi_N(\vec{r}_N) \end{vmatrix}$$

For relativistic case independent orbitals are Dirac's orbitals

$$\phi(\vec{r}_a) = \frac{1}{r} \begin{pmatrix} iP_a(r)\Omega_{\kappa_a m_a}(\hat{r}) \\ Q_a(r)\Omega_{-\kappa_a m_a}(\hat{r}) \end{pmatrix}$$

COUPLED CLUSTER/ALL ORDER METHOD

In coupled-cluster method, the exact **many-body wave function** is represented as

$$\left|\Psi_v\right\rangle = \exp(S)\left|\Psi_v^{(0)}\right\rangle \longrightarrow$$

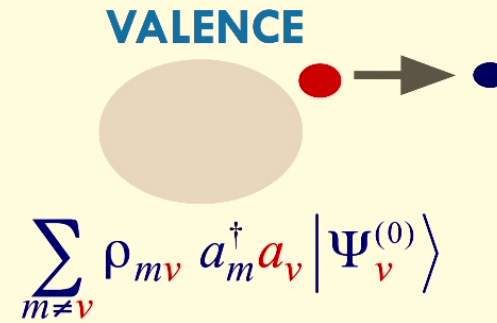**Lowest-order wavefunction**
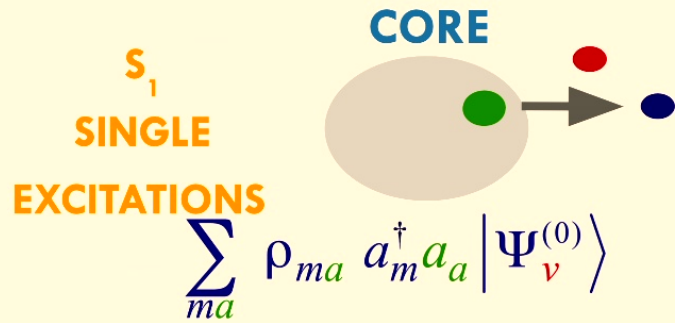
$$S = S_1 + S_2 + S_3 + \ldots + S_N$$

Expansion of **exponential**:

$$\left|\Psi_v\right\rangle = (1 + S_1 + S_2 + S_3 + \frac{1}{2}S_1^2 + S_1 S_2 + \frac{1}{2}S_2^2 + \ldots)\left|\Psi_v^{(0)}\right\rangle$$
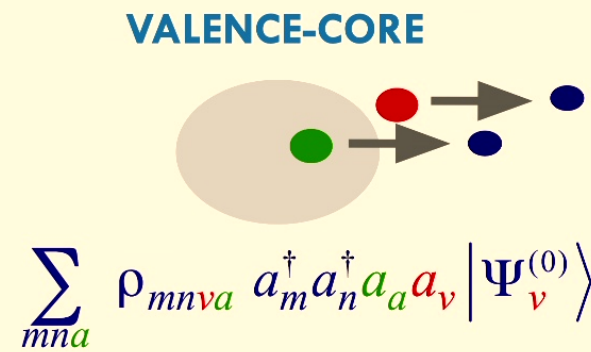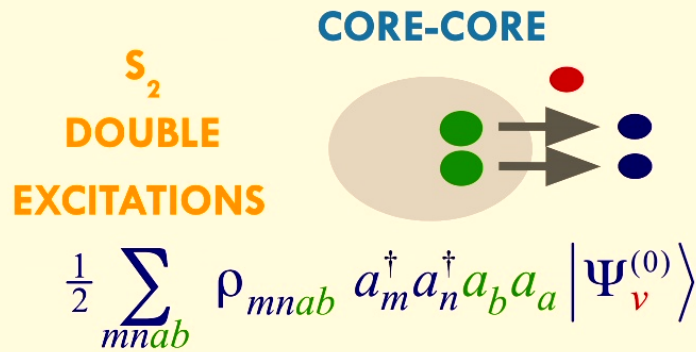
Linearized coupled cluster method restricted to single-double excitations

Blundell et al., Phys. Rev. A 40, 2233 (1989)

SINGLE DOUBLE WAVEFUNCTION

S$_1$
SINGLE
EXCITATIONS

CORE

$$\sum_{ma} \rho_{ma}\, a_m^\dagger a_a \left| \Psi_v^{(0)} \right\rangle$$

VALENCE

$$\sum_{m \neq v} \rho_{mv}\, a_m^\dagger a_v \left| \Psi_v^{(0)} \right\rangle$$

ρ_{ma}, ρ_{mv} are the single core & valence excitation coefficients

S$_2$
DOUBLE
EXCITATIONS

CORE-CORE

$$\frac{1}{2}\sum_{mnab} \rho_{mnab}\, a_m^\dagger a_n^\dagger a_b a_a \left| \Psi_v^{(0)} \right\rangle$$

VALENCE-CORE

$$\sum_{mna} \rho_{mnva}\, a_m^\dagger a_n^\dagger a_a a_v \left| \Psi_v^{(0)} \right\rangle$$

ρ_{mnab}, ρ_{mnva} are the double core & valence excitation coefficients

● core   ● valence electron   ● any excited orbital

ATOMIC PROPERTIES

$$\rho_{ma} \quad \rho_{mnab} \quad \rho_{mv} \quad \rho_{mnva}$$

$$Z_{wv}^{E1} = \frac{\langle \Psi_w | E1 | \Psi_v \rangle}{\sqrt{\langle \Psi_w | \Psi_w \rangle \langle \Psi_v | \Psi_v \rangle}}$$

Accurate "**database**" of over 5500 matrix elements for alkali-metal atoms and alkaline earth ions!

- Matrix Elements
- Line Strength
- Transition Probability
- Oscillator Strength
- Radiative Lifetime
- Frequency Shifts
- Dipole Polarizability
- Dispersion Interaction
- Magic Wavelengths
- Tune-out Wavelengths

SIGNIFICANT RESULTS

Hosted by the University of Delaware

- Accessible at udel.edu/atom

Free and open to all users
Supported Atomic Elements

- Neutral & Ionized:
  - Li, Be+, Na, Mg, Mg+, K, Ca, Ca+, Rb, Sr, Sr+, Cs, Ba+, Fr, Ra+
- Highly Ionized:
  - Cs6+, Ba7+, Ce9+, Pr10+, Nd11+–Nd13+, Sm13+–Sm15+, Eu14+, Cf15+, Cf17+

Atomic Properties

- Energies, matrix elements, branching ratios, transition rates, lifetimes
- Quadrupole moments, hyperfine constants
- Dynamic/static polarizabilities, magic wavelengths, magic zero wavelengths

Nuclear Data

- Includes isotope, half-life, natural abundance (%), nuclear spin
- RMS radii, magnetic and quadrupole moments
- Regular updates from latest sources

METRIC

Portal Access Statistics (via Google Analytics)

- **Since release (April 2021):**
  - 5,000+ users from 95 countries
  - 11,400 sessions
  - 81K pageviews (30K in past year)
- **Past year breakdown:**
  - 45% users from the U.S.
  - 8% from Germany
  - 6% each from India and the UK

Version 3 Updates

- New data: Extensive Mg, Sr, and Ba datasets
- Focused on high experimental interest areas

P. Barakhshan, A. Bhosale, A. Kiruga, R. Eigenmann, M. S. Safronova, B.Arora https://doi.org/10.48550/arXiv.2212.10665

SHIFT IN ENERGY LEVEL

Interaction between the dipole and the electric field

$$H_{\text{int}}^{D} = -\varepsilon\,(t).D$$

Interaction between the quadrupole and the gradient of electric field

$$H_{\text{int}}^{Q} = -\nabla\varepsilon\,(t).Q$$

Second-order perturbation theory

$$\Delta E^{v} = -\frac{1}{4}\alpha_{D}^{v}(\omega)\,\varepsilon^{2} - \frac{1}{16}\alpha_{Q}^{v}(\omega)\,\nabla\varepsilon^{2} - \ldots\ldots$$
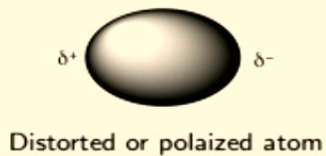
Dipole Polarizability   **Quadrupole Polarizability**

POLARIZABILITY

The ease with which the distortion can take place

$$\alpha_J = \alpha_J^{(0)}(\omega) + \frac{A\cos\theta_k M_J}{2J}\alpha_J^{(1)}(\omega) + \left(\frac{3\cos^2\theta_p - 1}{2}\right)\frac{3M^2 - J(J+1)}{J(2J-1)}\alpha_J^{(2)}(\omega)$$

Neutral atom

δ^+ δ^-

Distorted or polaized atom

$$\alpha^v(\omega) = \sum_n A(j_v)\frac{(E_n - E_v)\left|\langle n\|D\|v\rangle\right|^2}{(E_n - E_v)^2 - \omega^2}$$

Electric-dipole reduced matrix element, CALCULATE

Sum over **intermediate states**
n converges very fast

Energy values (known very well)

$$\alpha^v = \alpha^v_{main} + \alpha^v_{tail}$$

$$\alpha_{total} = \alpha^v_{main} + \alpha^v_{tail} + \alpha_{core}$$

CONTRIBUTIONS TO THE 6S$_{1/2}$ SCALAR POLARIZABILITY (Cs)
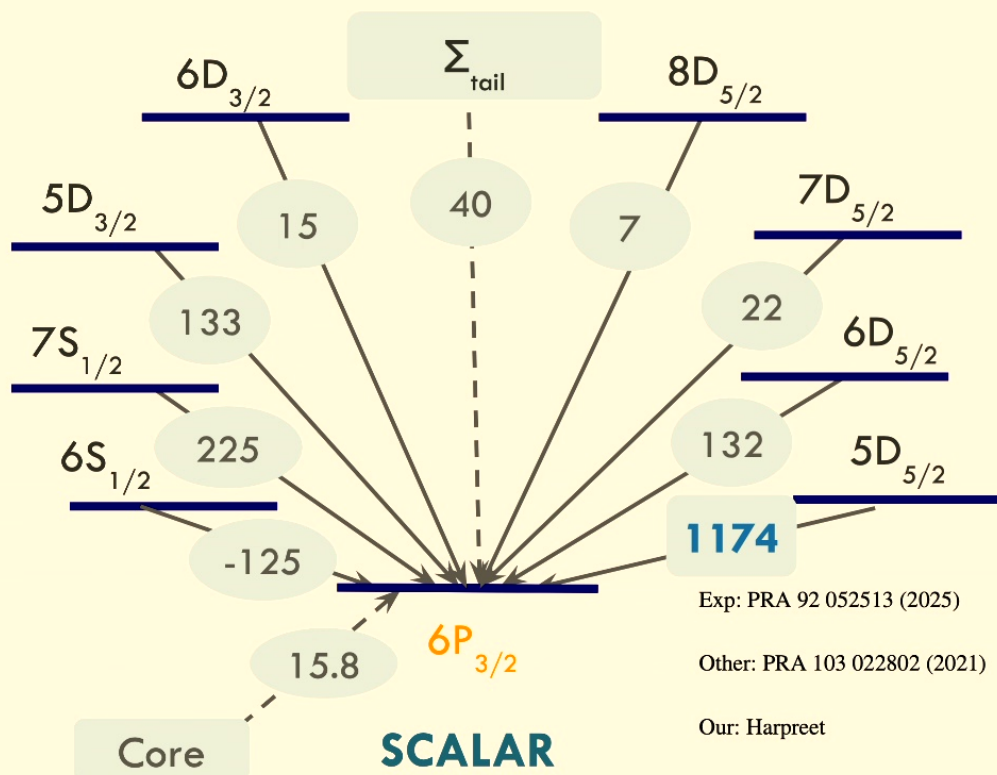

$$\alpha_{total} = \alpha^v_{main} + \alpha^v_{tail} + \alpha_{core}$$

$$\alpha^v(\omega) = \sum_n A(j_v) \frac{(E_n - E_v)\left|\langle n\|D\|v\rangle\right|^2}{(E_n - E_v)^2 - \omega^2}$$

8p$_{3/2}$ Tail 8p$_{1/2}$

0.2   0.3   0.2

7p$_{3/2}$ 7p$_{1/2}$

0.6   0.3

6p$_{3/2}$ 6p$_{1/2}$

250   132

6s
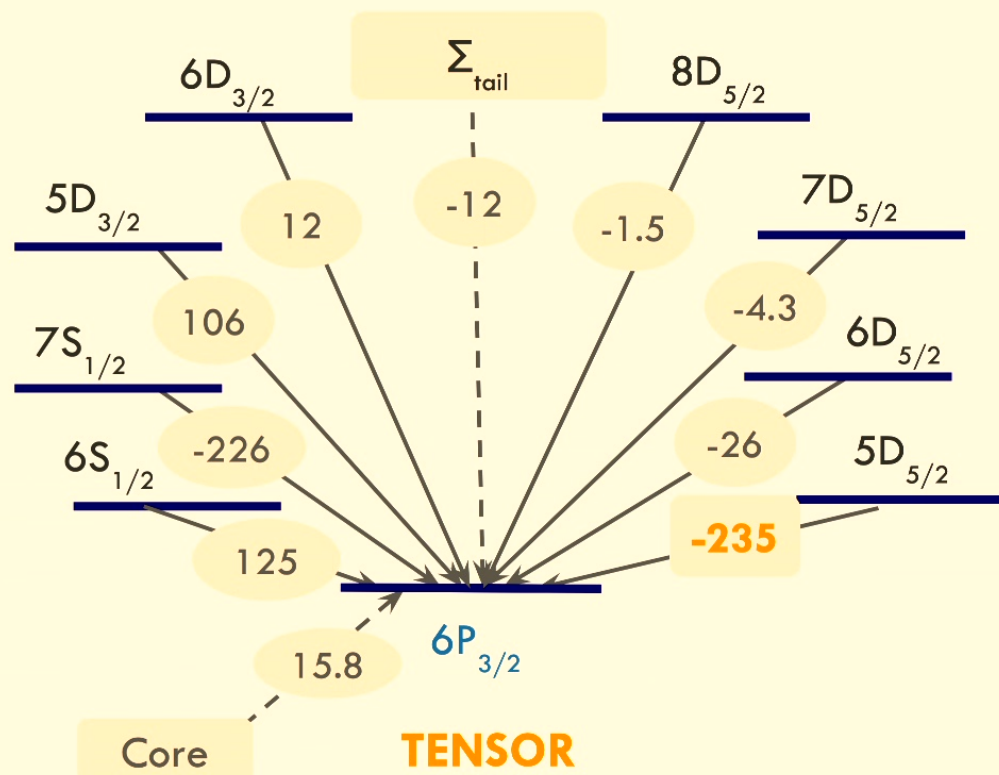
15.8
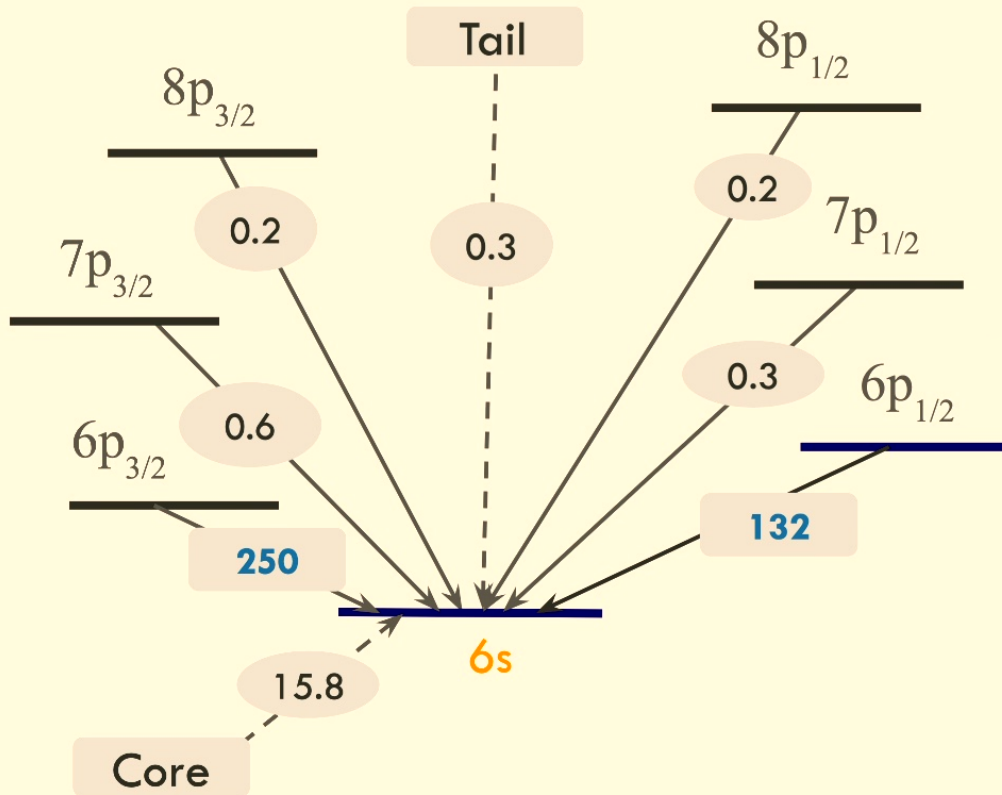
Core

Our (a.u.)	Other	Exp
399.7(8)	391.1	400.8(4) 401.0(6)

S. Singh, B. Arora, B. K. Sahoo, JPB 49 (2016)
Exp: PRA 92 052513 (2015), PRL 91 153001 (2003)
Other: PRA 103 022802 (2021)

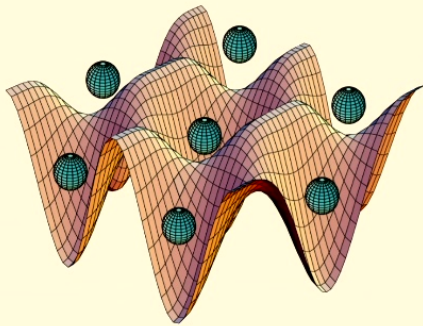# CONTRIBUTIONS TO THE 6P$_{3/2}$ POLARIZABILITY (Cs)

Exp: PRA 92 052513 (2025)

Other: PRA 103 022802 (2021)

Our: Harpreet

SCALAR

Our (a.u.)	Other	Experiment
1644(13)	1650	1641(2)

TENSOR

Our (a.u.)	Other	Experiment
-262(2)	-261	-262(2)

OPTICAL DIPOLE TRAPS

Trapping of atoms in optical lattices

- In optical dipole trap, a force arises from the interaction of the induced atomic dipole moment with the intensity gradient of the light field.

- **Trapping potential depends on state of atom.**
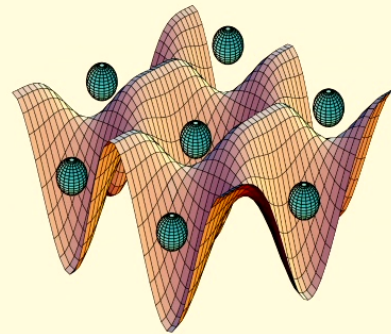
$$U \propto \Delta E(\omega) \text{ or } \alpha(\omega)$$

is state dependent

STATE INSENSITIVE TRAPPING

Magic wavelength λ_{magic} is the wavelength for which the optical potential U experienced by an atom is independent on its state

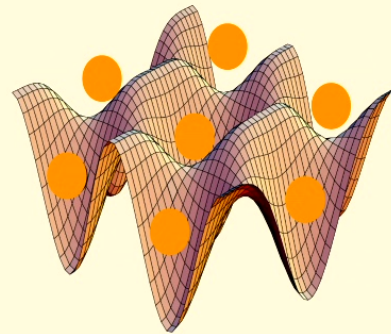

Atom in state A
sees potential U_A

$$U \propto \Delta E(\omega) \text{ or } \alpha(\omega) \longrightarrow \text{ac polarizability}$$

Need electric-dipole polarizability α to determine how deep the trap will be for specified laser wavelength for atom in an atomic state

STATE INSENSITIVE TRAPPING

Magic wavelength λ_{magic} is the wavelength for which the optical potential U experienced by an atom is independent on its state

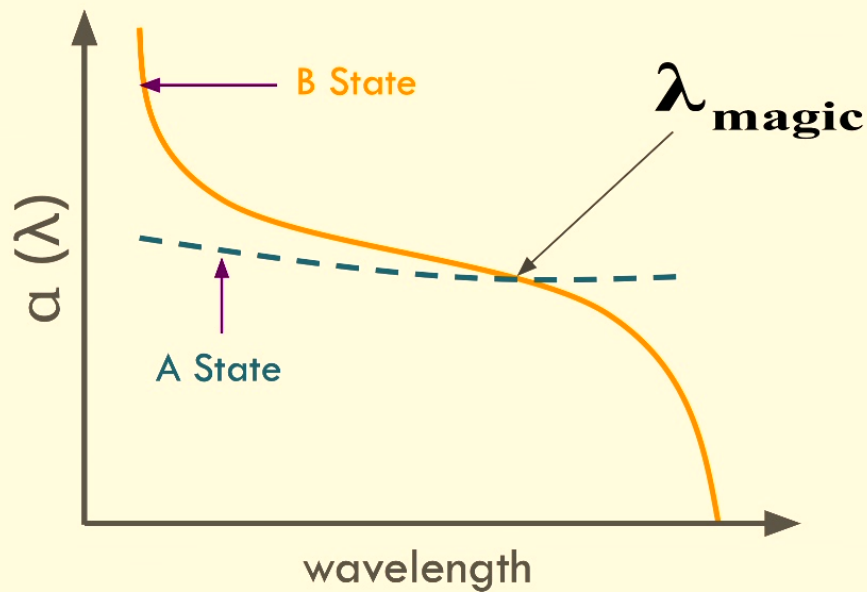**Atom in state B sees potential U_B**

$$U \propto \Delta E(\omega) \text{ or } \alpha(\omega) \longrightarrow \text{ac polarizability}$$

Need electric-dipole polarizability α to determine how deep the trap will be for specified laser wavelength for atom in an atomic state

MAGIC WAVELENGTH

Magic wavelength λ_{magic} is the wavelength at which the polarizability for both the states cross
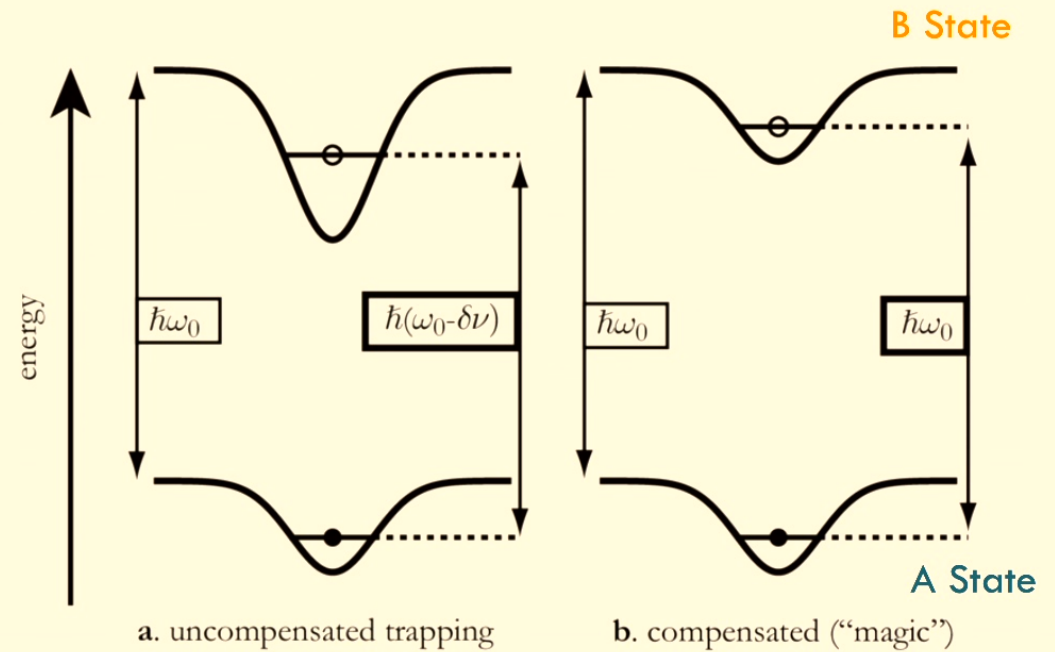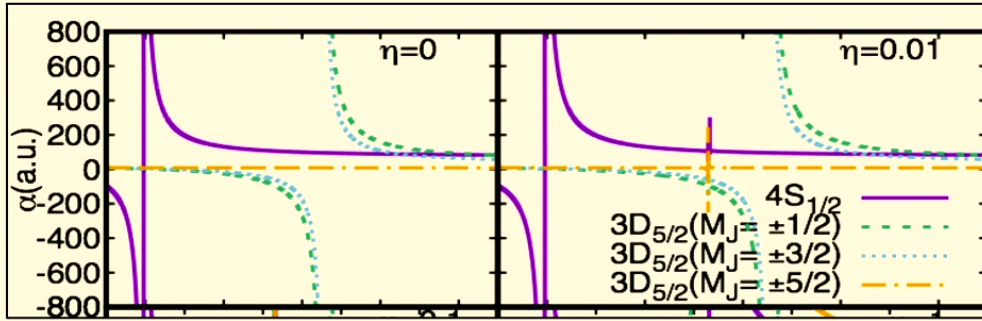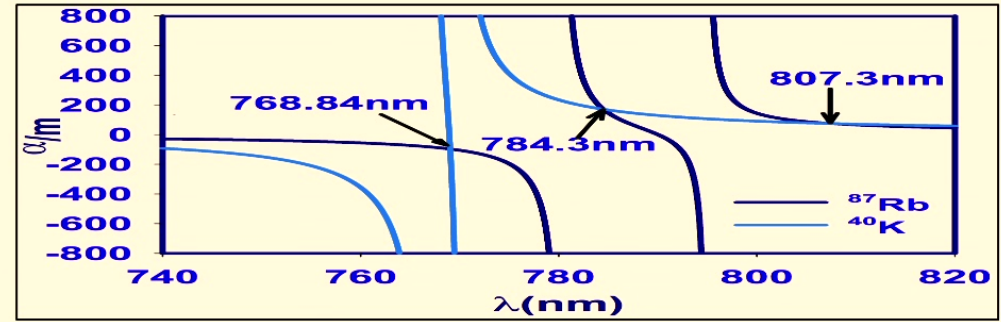

Katori et al. Phys. Rev. Lett. 103, 153004 (2009)

a. uncompensated trapping   **b.** compensated ("magic")
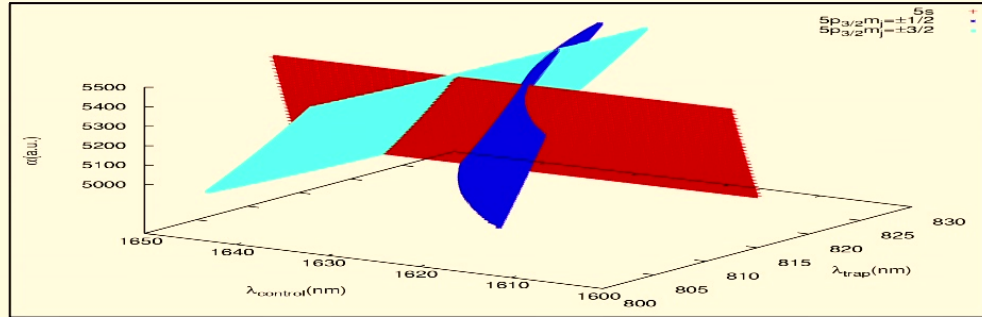
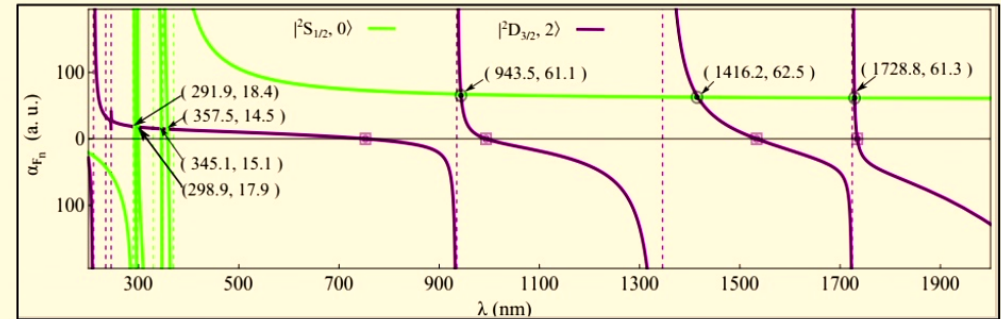Image source: Lundblad, Nathan & Schlosser, M. & Porto, J.

Atoms@GNDU

Magic wavelengths

$\eta=0$

$\eta=0.01$

$4S_{1/2}$
$3D_{5/2}(M_J=\pm1/2)$
$3D_{5/2}(M_J=\pm3/2)$
$3D_{5/2}(M_J=\pm5/2)$

Simultaneous trapping for two systems

768.84nm
784.3nm
807.3nm

^{87}Rb
^{40}K

λ(nm)

Two-color optical trapping

5s
$5p_{3/2}m_j=\pm1/2$
$5p_{3/2}m_j=\pm3/2$

$\lambda_{control}$(nm)
λ_{trap}(nm)

Magic-zero wavelengths

$|^2S_{1/2},0\rangle$
$|^2D_{3/2},2\rangle$

(291.9, 18.4)
(357.5, 14.5)
(345.1, 15.1)
(298.9, 17.9)
(943.5, 61.1)
(1416.2, 62.5)
(1728.8, 61.3)

λ (nm)

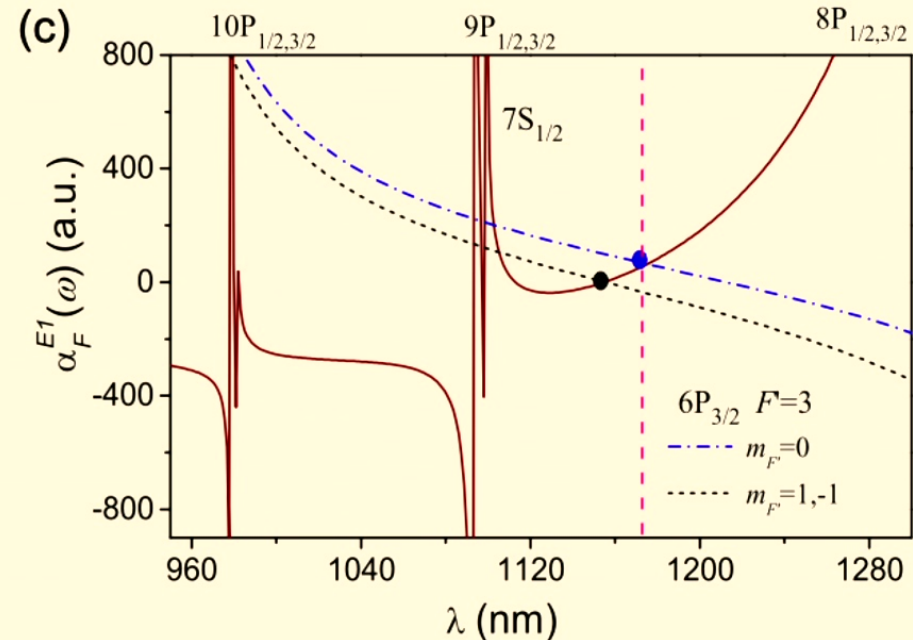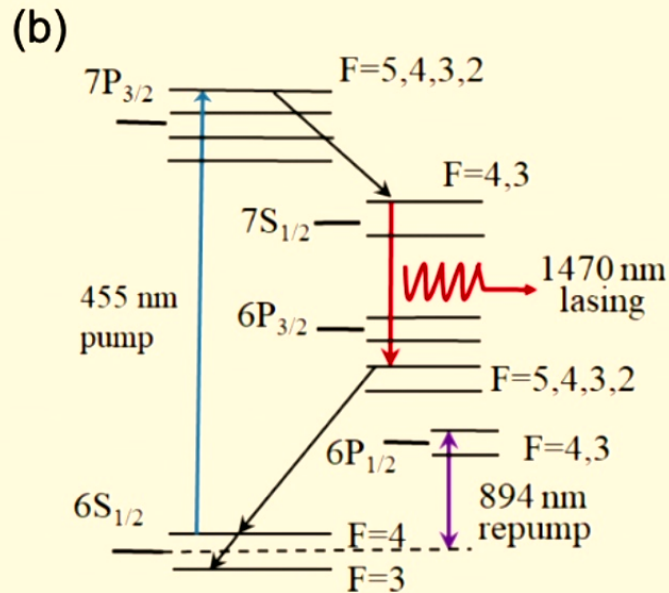**Jasmeet Kaur**   **Sukhjit Singh**   **Kiranpreet Kaur**   **Maninder Kaur**   **Mandeep Kaur**   **Harpreet Kaur**   **Jyoti Arora**   **Vipul Badhan**

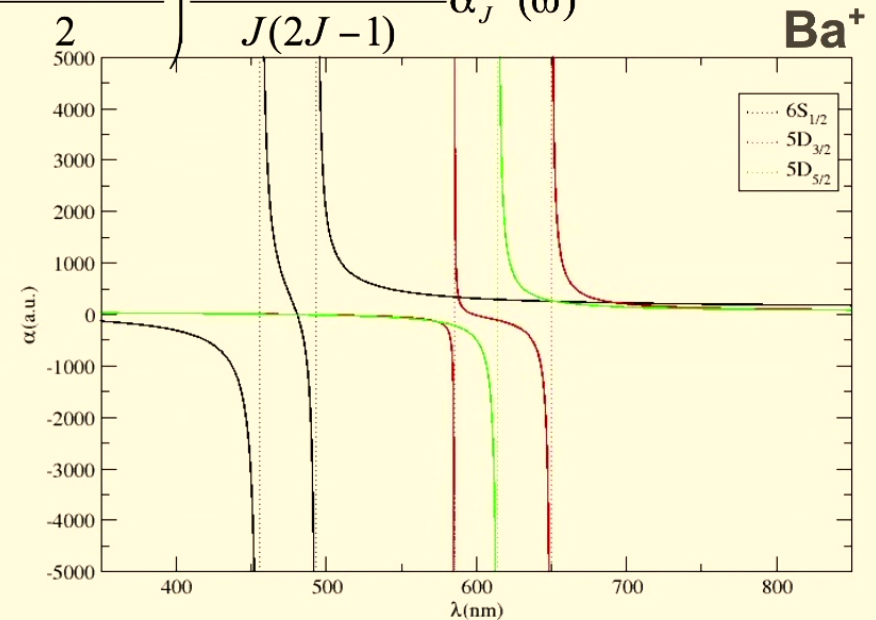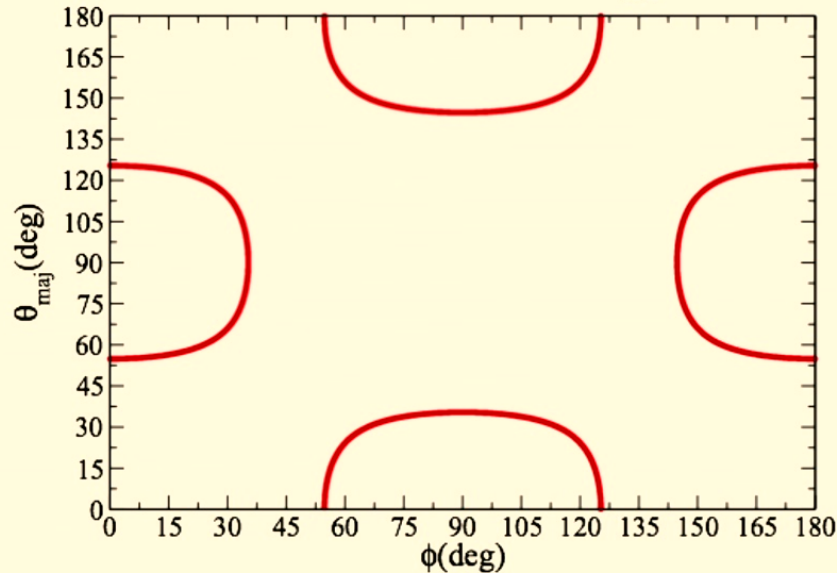# MAGIC WAVELENGTHS FOR EXCITED STATES

F-dependent dynamic polarizabilities (in a.u.) of $|7S_{1/2}; F = 4, M_F = 0\rangle \rightarrow |6P_{3/2}; F = 3, M_F = 0\rangle$ clock transition of Cs for linearly polarized light.

Needed for new class of (active) atomic clocks

D. Pan, B. Arora, Y. Yu, B. K. Sahoo, J. Chen PRA 102, 041101(R)(2020)

COMPREHENSIVE OPTICAL TRAPPING

$$\alpha_J = \alpha_J^{(0)}(\omega) + \frac{A\cos\theta_k M_J}{2J}\alpha_J^{(1)}(\omega) + \left(\frac{3\cos^2\theta_p - 1}{2}\right)\frac{3M^2 - J(J+1)}{J(2J-1)}\alpha_J^{(2)}(\omega)$$

Ba⁺

- θ_k is the angle between propagation vector k and quantization axis e_B

- Angle θ_p depends on Φ (measure of polarization) and angles θ_{min} and θ_{maj} angles between e_B and semimajor ε_{maj} and semiminor ε_{min} axes of the ellipse swept by the elliptically polarized electric field

S. Singh, B.K. Sahoo, B. Arora PRA 93, 063411 (2016), Jyoti, H. Kaur, B. Arora, B. K. Sahoo Atoms 10(3) (2022)

ATOMIC CLOCKS

An atomic clock is a type of clock that uses an atomic resonance frequency standard as its timekeeping element

Ultrastable laser

Atomic transition

$E = \frac{hc}{\lambda}$

Atomoic excitation

$E = \frac{hc}{\lambda}$
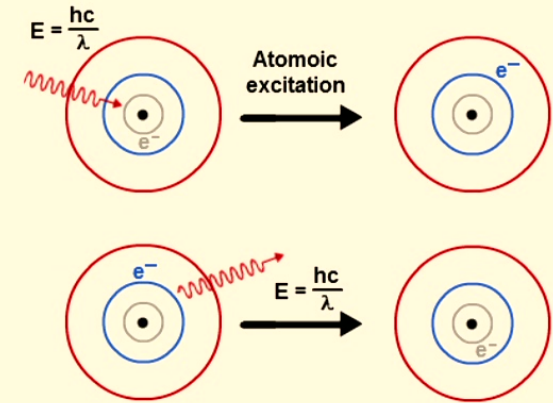
BASIC IDEA: TUNE THE LASER TO THE FREQUENCY OF THE ATOMIC TRANSITION

Image source: Atomic Physics group at UDel

CURRENT DEFINITION

The second is the duration of **9192631770** periods of the radiation corresponding to the hyperfine transition between two hyperfine levels of the ground state of the Cs 133 atoms (at 0K).
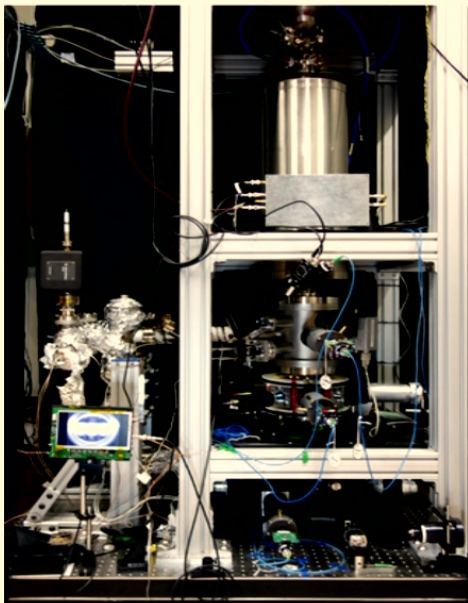

NIST-F3 cesium fountain
frequency reference

F=4 ------------

9.2 GHz

F=3 ------------

Will neither gain nor lose a second in 300 million years (fractional frequency uncertainty 10^{-16})

linewidth

$$\sigma_y(\tau) \approx \frac{\Delta\nu}{\nu_0\sqrt{N}}\sqrt{\frac{T_c}{\tau}}$$

instability

Transition frequency
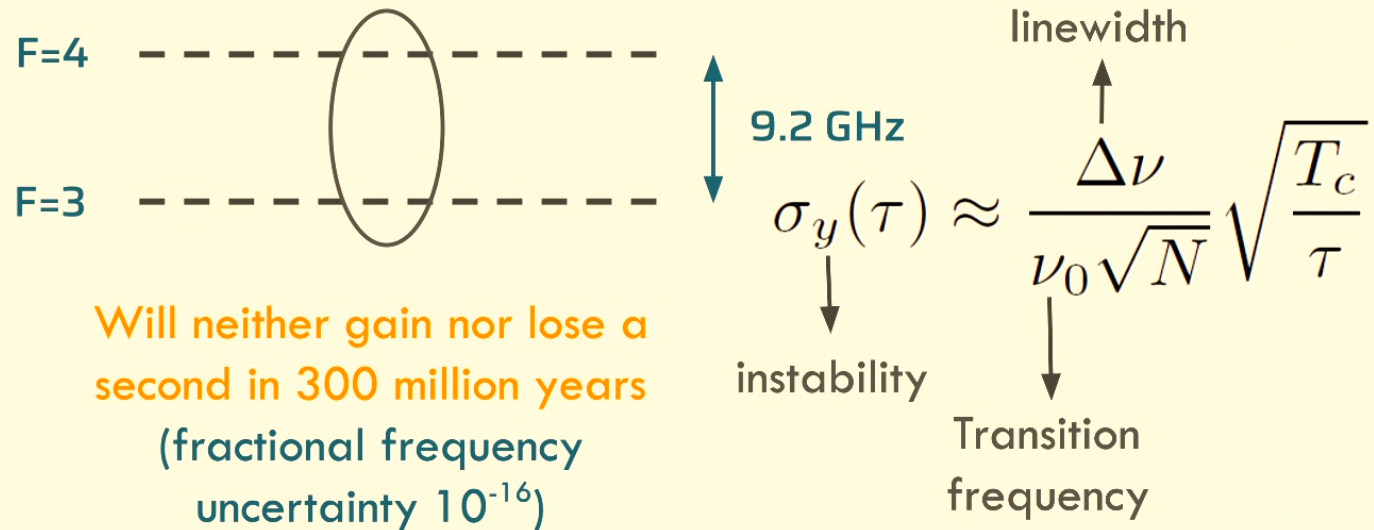
How well repeated measurements produce the same time intervals.

BETTER CLOCKS-Precision & Stability

What ticks faster than Cs?

Image source: ChatGPT

BETTER CLOCKS

Build different clocks:

optical clocks, highly charged ion clocks, nuclear clocks, molecular clocks

$4p_{3/2}$

$4p_{1/2}$

854 nm $\big\}$ Easily produced by non-bulky solid state or diode laser

866 nm

$3d_{5/2}$ Lifetime $\cong$ 1.2 s

$3d_{3/2}$

393 nm cooling

397 nm

732 nm

E 2

729 nm Clock transition

$4s_{1/2}$

Ca$^+$ Clock transition - $3d_{5/2} \rightarrow 4S_{1/2}$

Fractional frequency uncertainty vs Year. ▲ Microwave clocks, ● Optical clocks.
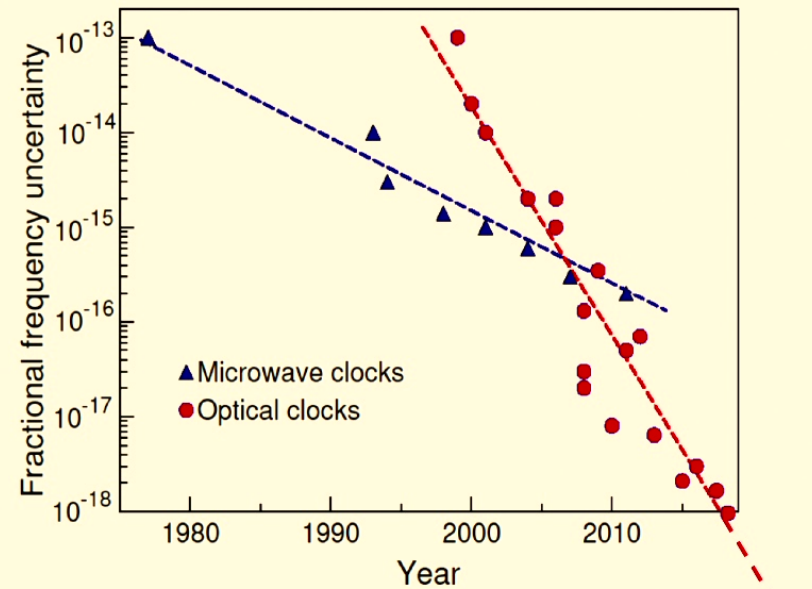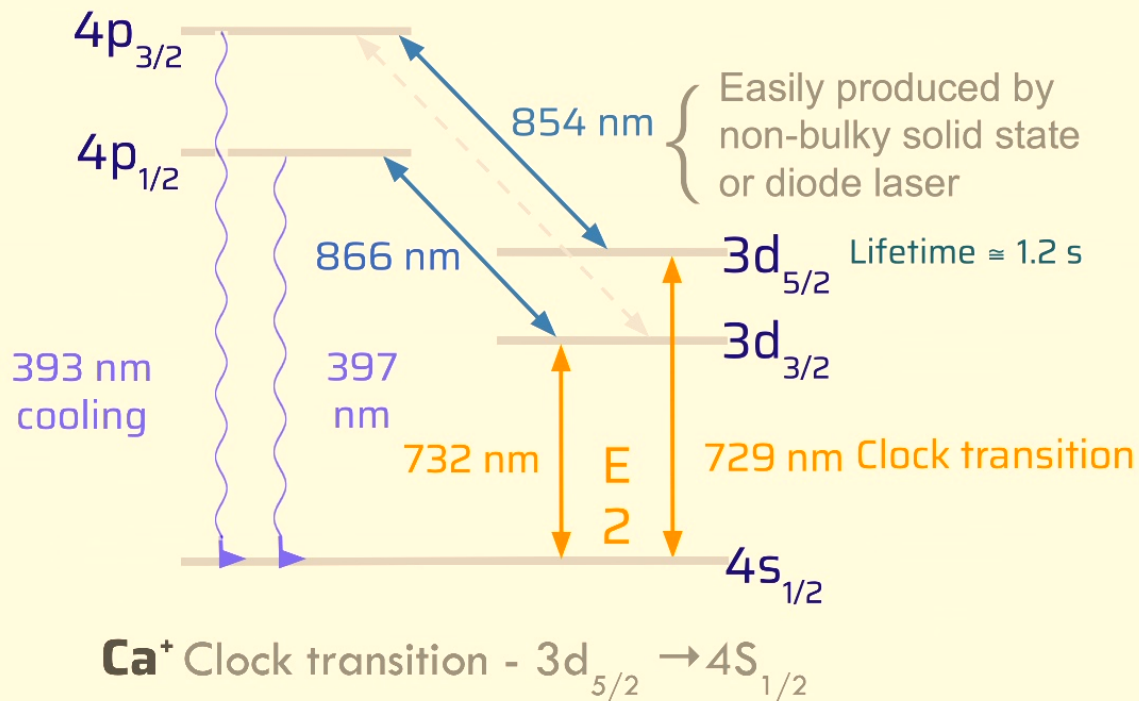
TERAHERTZ CLOCKS

Clock transition lies in TeraHz region

High frequency $\Rightarrow$ High stability
Small linewidth $\Rightarrow$ high stability

THz clock transition between $4D_{3/2}$ and $4D_{5/2}$ states of Zr^{3+} at **37.52 THz** with a wavelength of $7.9955 \mu m$

Lifetime of $4D_{5/2}$ is **47.38 s** allowing for population inversion
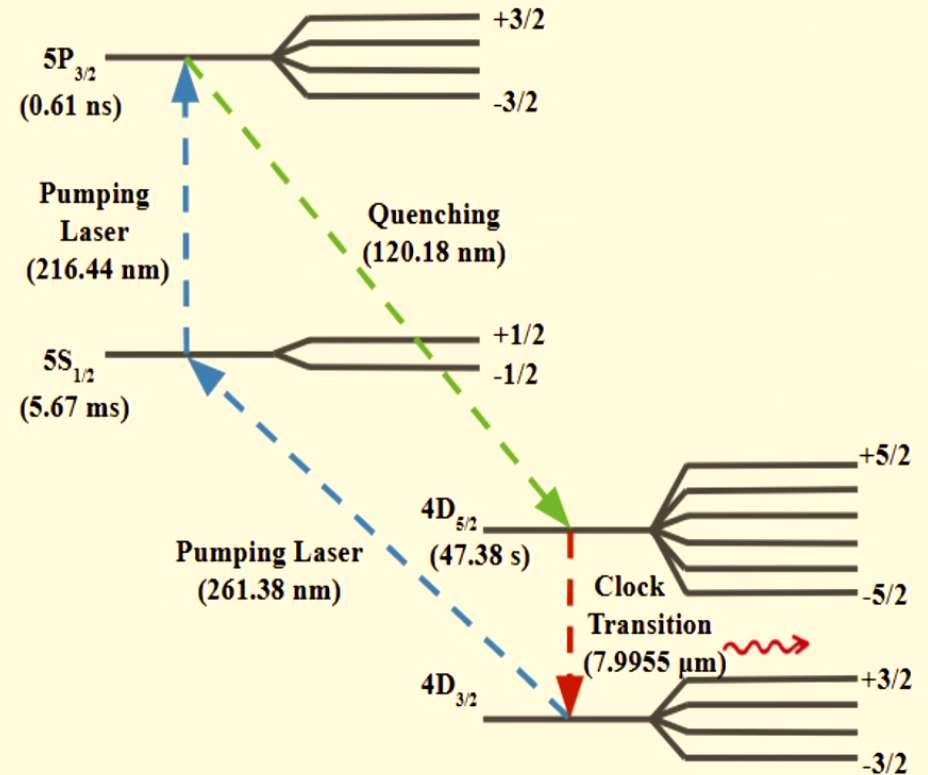
Jyoti, A. Chakraborty,, Y.Yu, J. Chen6, B. Arora, B. K. Sahoo Phys. Rev. A 108, 023115 (2023)
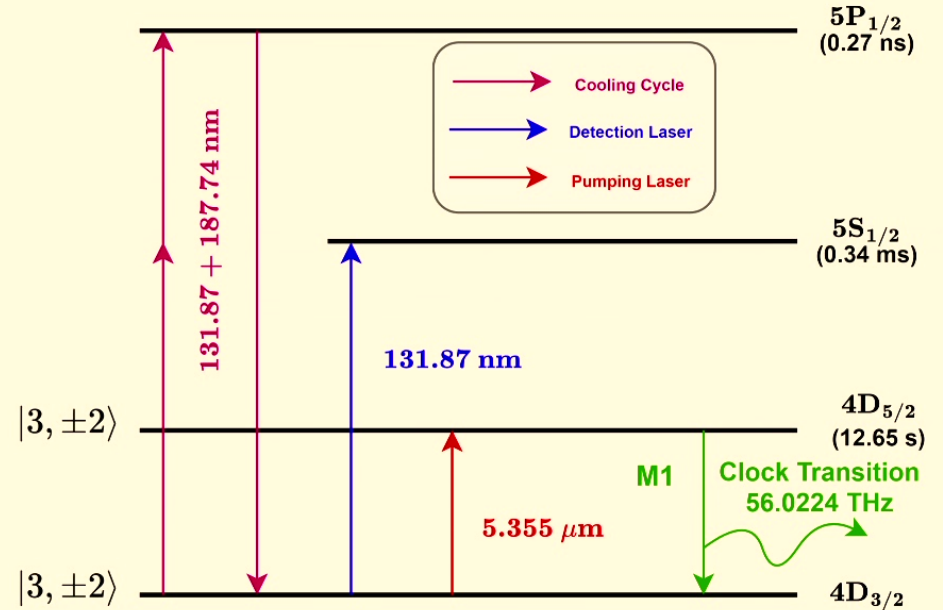
FOUNTAIN TERAHERTZ CLOCKS

Clock transition lies in TeraHz region

^{93}Nb- almost 100% natural abundance

THz clock transition between
$4D3/2|3,\pm2\rangle$–$4D5/2|3,\pm2\rangle$ states of **Nb^{4+}** at
56.0244 THz with a wavelength of 5.355μm

Lifetime of **$4D_{5/2}$ is 12.65 s** allowing for population inversion

No electric quadrupole shifts or ac stark shift of levels due to pumping laser

Cooling Cycle
Detection Laser
Pumping Laser

$5P_{1/2}$ (0.27 ns)
$5S_{1/2}$ (0.34 ms)
$4D_{5/2}$ (12.65 s)
$4D_{3/2}$

131.87 + 187.74 nm
131.87 nm
5.355 μm
M1
Clock Transition 56.0224 THz
$|3,\pm2\rangle$
$|3,\pm2\rangle$

Jyoti, A. Chakraborty, J. Chen, B. Arora, and B. K. Sahoo (PRA under review)

IDEAL DEFINITION

$$v_{clock} = v_o$$

Clock transition

EXTERNAL PERTURBATION
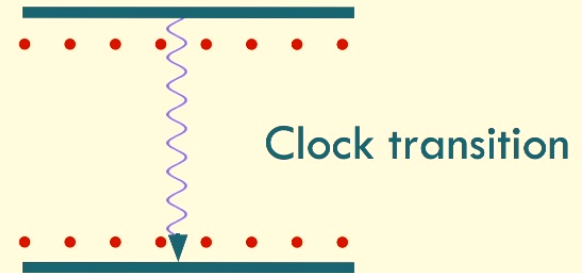
$$v_{clock} = v_o + \Delta v_p$$

Clock transition

Transition frequency should be corrected to
account for the effect of the external perturbation

SYSTEMATIC ERRORS

Due to change in energy levels from external perturbations

Magnetic field

Electric field

Thermal field

Collisions

Field gradient

Gravitational Field

→

Zeeman Shift

Quadratic Stark Shift(AC/DC)

Blackbody Radiation Shift

Doppler Shift

Quadrupole Shift

Gravitational Red Shift

SYSTEMATIC ERRORS

Due to change in energy levels from external perturbations

Temperature dependent electromagnetic fields created by blackbody

$$\frac{3}{8\pi} E_l^2(\omega) = \frac{3}{8\pi} B_l^2(\omega) = \frac{1}{\pi^2 c^3} \frac{\omega^3}{\exp(\omega/K_B T - 1)}$$

Frequency shift caused by **black body radiations**

$$\Delta\upsilon_{BBR}^{\lambda,L} = -\frac{1}{2}\left\langle E^2(\omega)/B^2(\omega)\right\rangle \alpha_0^{\lambda,L}$$

Static multipolar polarizability

Frequency shift caused due to **pumping laser**

$$\Delta\nu_{\text{Stark}} = -\frac{1}{2\pi}\left(\frac{\mathcal{E}}{2}\right)^2 \Delta\alpha^{E1}$$

Frequency shift caused due to **electric field gradients**

$$\Delta\nu_{EQ} = -\frac{1}{2h}\Delta\Theta\frac{\partial\mathcal{E}_z}{\partial z}$$

Electric quadrupole moment

MULTIPOLAR POLARIZABILITY/MOMENTS Zr^{3+}

Shifts	4D$_{3/2}$	4D$_{5/2}$	
BBR shift (Stark)	5.0708 a.u.	4.8432 a.u.	Static electric dipole α
BBR shift (Zeeman)	1.3940×10^{-27} JT^{-2}	-9.2925×10^{-28} JT^{-2}	Static magnetic dipole α
Quadratic Stark	0.7278 a.u.	0.8426 a.u.	Quadrupole moment
AC Stark (216.44 nm)	7.1374 a.u.	7.0575 a.u.	Dynamic electric dipole α
AC Stark (261.38 nm)	6.7386 a.u.	6.6615 a.u.	Dynamic electric dipole α

DIFFERENT SYSTEMATIC SHIFTS

4D3/2-4D5/2 CLOCK TRANSITION IN Zr^{3+}ION

Source	$\Delta\nu$ (Hz)	$\frac{\Delta\nu}{\nu_0}$
AC Stark (261.38 nm)	7.64×10^{-9}	2.04×10^{-22}
AC Stark (216.44 nm)	7.91×10^{-9}	2.11×10^{-22}
Quadratic Zeeman (B=10^{-8} T)	2.26×10^{-9}	6.03×10^{-23}
Electric Quadrupole ($\frac{\partial\mathcal{E}}{\partial z} = 10^6 V/m^2$)	-0.52	-1.39×10^{-14}
BBR Stark (T=300 K)	1.96×10^{-3}	5.22×10^{-17}
BBR Zeeman (T=300 K)	1.74×10^{-4}	4.63×10^{-18}

4D3/2-4D5/2 CLOCK TRANSITION IN Nb^{4+}ION

Source	$\Delta\nu$ (Hz)	$\frac{\Delta\nu}{\nu_0}$
Electric Quadrupole	0	0
BBR Zeeman (T=300 K)	-0.3928	-7.0115×10^{-15}
BBR Stark (T=300 K)	-6.9743×10^{-5}	-1.2449×10^{-18}
Quadratic Zeeman (B=10^{-8} T)	-5.1197×10^{-6}	-9.1387×10^{-20}

- Quadrupole shifts can be average out to zero experimentally
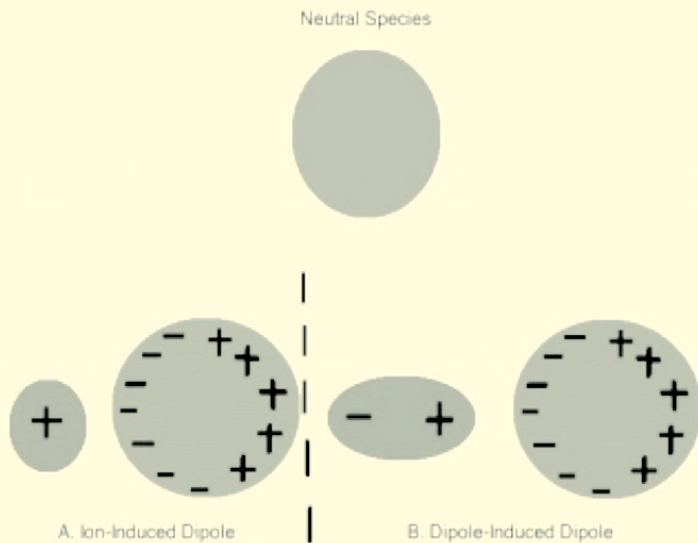- Nuclear spin=0, no hyperfine levels

- Pumping and cooling lasers are shut down during the clock transition
- Choice of 4D3/2|3,±2⟩–4D5/2|3,±2⟩ leads to zero quadrupole shits

Linear Zeeman shift can be avoided if average is taken over the transition frequencies with positive and negative M_F states

ATOM-ATOM (-ATOM) INTERACTION

Presence of a dipole or ion nearby a neutral atom can induce dipole in a neutral atom

Neutral Species

A. Ion-Induced Dipole   B. Dipole-Induced Dipole

Knowledge of dispersion interaction of atoms with atoms are important in **hybrid traps, charge-exchange reactions, molecular formation and ultra cold atom-atom collision dynamics**

Short separations

$$U^a(R) = -\frac{C_6^{ab}}{R^6}$$

$$C_6^{ab} = \frac{1}{4\pi}\int_0^\infty d\omega\, \alpha^a(i\omega)\alpha^b(i\omega)$$
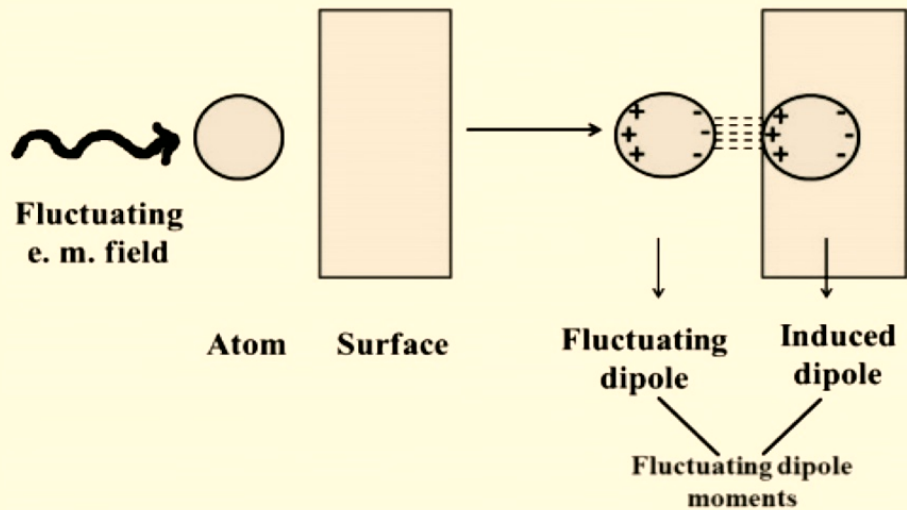
Intermediate separations

$$U^a(R) = -\frac{C_6^{ab}}{R^6}f_6^{ab}(R)$$

$$f_6^{ab} = \frac{1}{4\pi C_6^{ab}}\int_0^\infty d\omega\, \alpha^a(i\omega)\alpha^b(i\omega)e^{-2\alpha f_s \omega R}P(\alpha f_s \omega R)$$

ATOM-WALL INTERACTION

Dispersion Forces

Fluctuating e. m. field

Atom **Surface** **Fluctuating dipole** **Induced dipole**

**Fluctuating dipole moments**

Knowledge of dispersion interaction of atoms with bulk materials are important in **microelectronics, atom optics and atom interferometry experiments.**

Dynamic polarizability

$$U^a(R) = -\frac{1}{4\pi R^3} \int_0^\infty d\omega\, \alpha(i\omega) \frac{\varepsilon(i\omega) - 1}{\varepsilon(i\omega) + 1}$$

Dielectric permittivity

Arises as a result of interaction between atom and image dipole induced in the wall

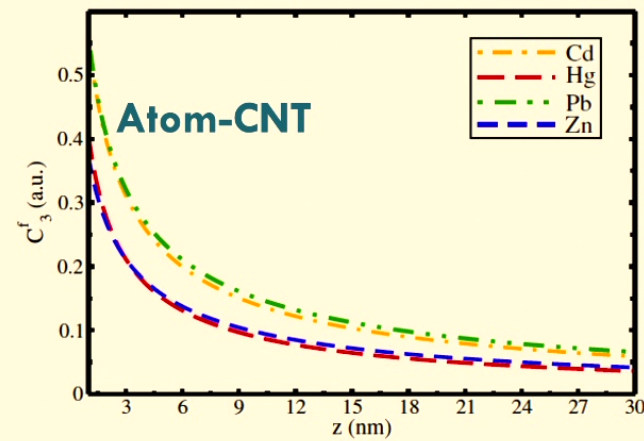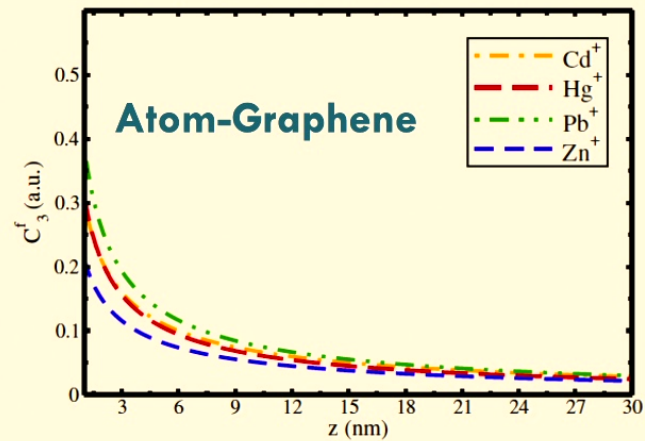# ATOM-CARBON NANOSTRUCTURE INTERACTION

Graphene Sheet

Carbon Nanotube

rolled up
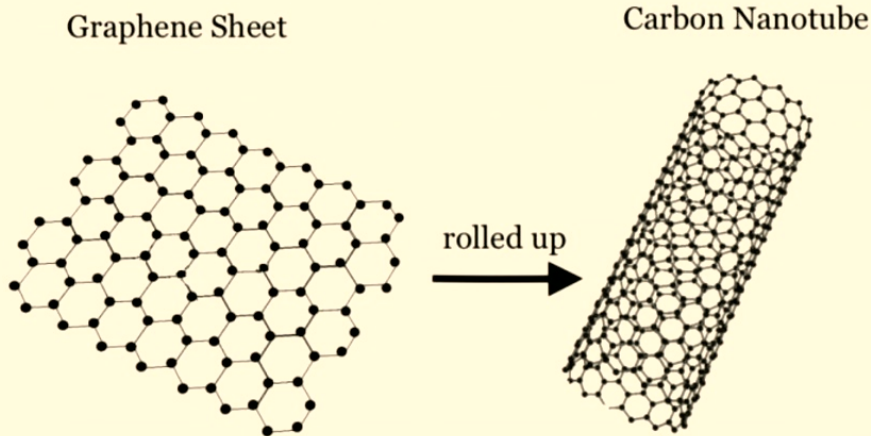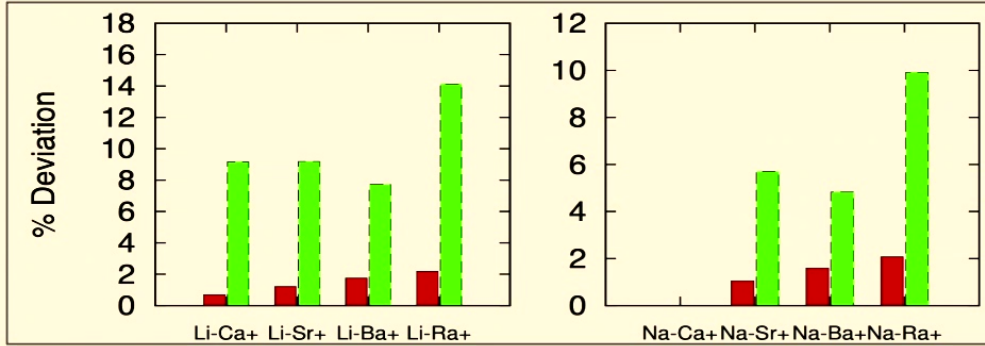
Dynamic polarizability

$$C_3(a,T) = -\frac{k_B T}{8} \sum_l{}' \alpha(i\zeta_l \omega_c) \int_{\zeta_l}^{\infty} dy\, e^{-y} \left[2y^2 \times r_{TM}(i\zeta_l, y)(-\zeta_l^2)\{ r_{TM} + r_{TE} \} \right]$$
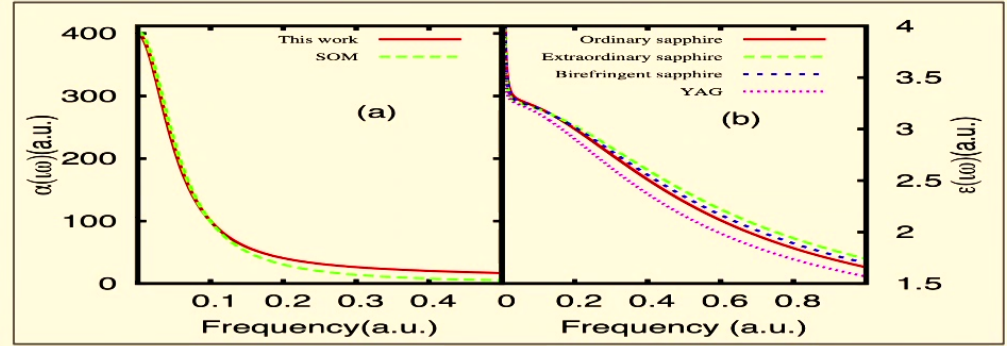
Reflection coefficients

Atom-Graphene

Cd$^+$
Hg$^+$
Pb$^+$
Zn$^+$

C_3^f (a.u.)

z (nm)

Atom-CNT

Cd
Hg
Pb
Zn

C_3^f (a.u.)

z (nm)

H. Kaur, N. Shukla, R. Srivastava, B. Arora, Phys. Rev. A **104**, 012806 (2021)
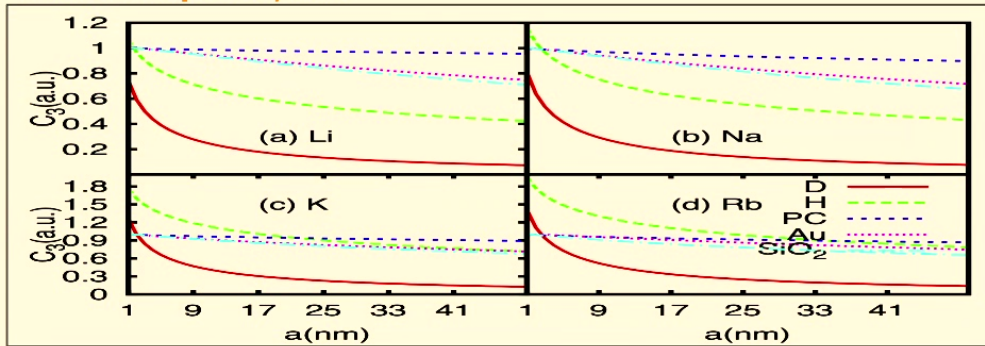
Atoms@GNDU

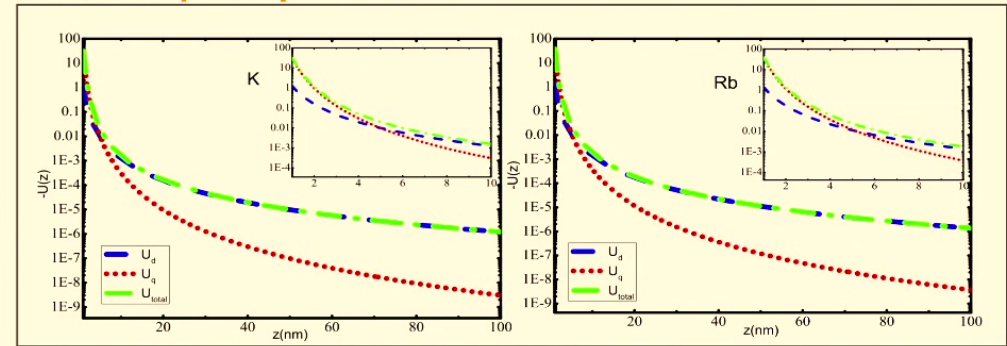## Atom-Atom(-Atom) interaction

Atom-Wall interaction

Atom-Graphene/CNT

Effect of quadrupole correction

Jasmeet Kaur   Sukhjit Singh   Kiranpreet Kaur   Maninder Kaur   Mandeep Kaur   Harpreet Kaur   Jyoti Arora   Vipul Badhan

CORRECTION DUE TO HIGHER ORDER TERMS

Total **interaction potential** arising from the fluctuating multipole moments of an atom interacting with its image in the surface

$$U_{total}(z) = U_d(z) + U_q(z) + \ldots \quad = -\frac{C_3}{z^3} - \frac{C_5}{z^5}$$

$$\frac{1}{4\pi} \int_0^\infty d\omega\, \alpha_q(\iota\omega) \frac{\epsilon_r(\iota\omega) - 1}{\epsilon_r(\iota\omega) + 1}$$

Total quadrupole polarizability in terms of tensor components

$$\alpha_n^q = \left[\alpha_n^{q(0)} - \alpha_n^{q(2)} \frac{3M_{J_n}^2 - J_n(J_n + 1)}{J_n(2J_n - 1)} - 3\alpha_n^{q(4)}(5M_n^2 - J_n^2 - 2J_n) \right. $$
$$\left. \times \frac{(5M_n^2 + 1 - J_n^2) - 10M_n^2(4M_n^2 - 1)}{J_n(J_n - 1)(2J_n - 1)(2J_n - 3)} \right]$$

S. Singh, M. Kaur, B. Arora, B. K. Sahoo Phys. Rev. A 98, 013406 (2018), H. Kaur, S. Singh, B. Arora, B. K. Sahoo Phys. Rev. A 105, 032819 (2022)
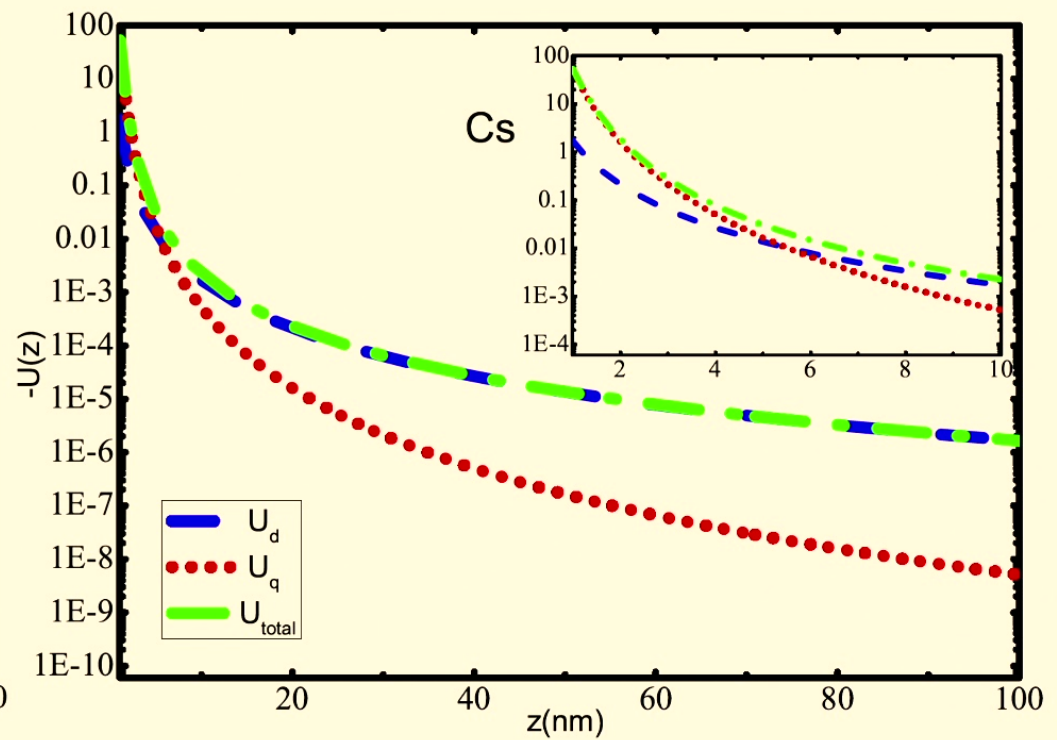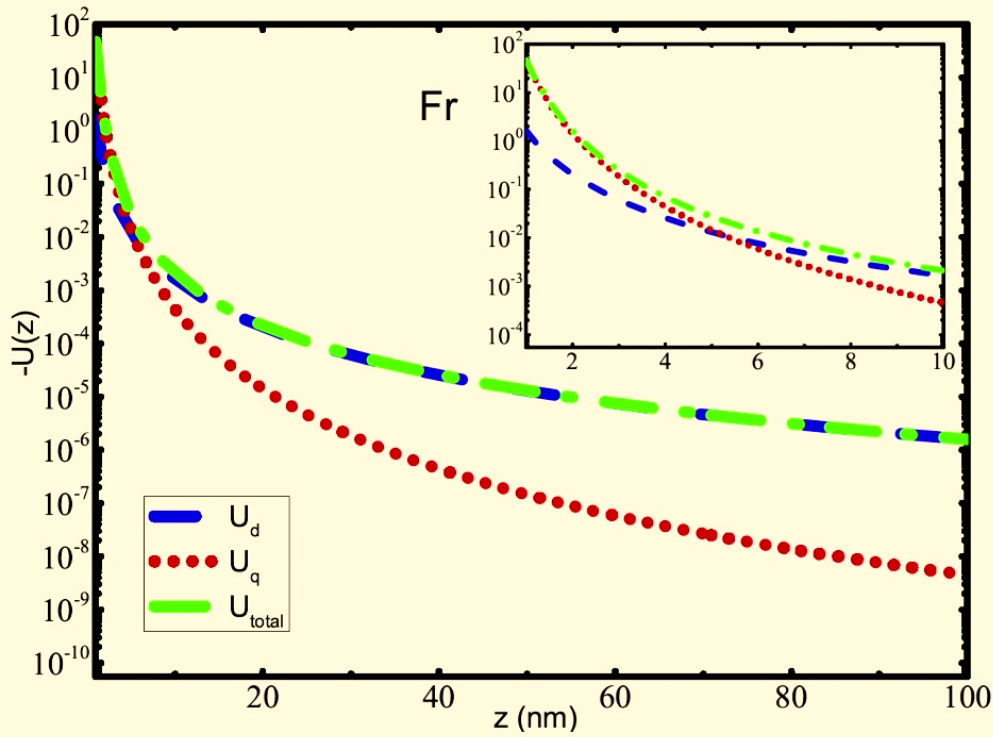
QUADRUPOLE POLARIZABILITY

Rb			Cs			Fr		
Contribution	E2	$\alpha_q(0)$	Contribution	E2	$\alpha_q(0)$	Contribution	E2	$\alpha_q(0)$
$\alpha_{q,Main}$			$\alpha_{q,Main}$			$\alpha_{q,Main}$		
$5S_{1/2}$ - $4D_{3/2}$	32.94	2461	$6S_{1/2}$ - $5D_{3/2}$	33.33	3362	$7S_{1/2}$ - $6D_{3/2}$	32.91	2930
$5S_{1/2}$ - $5D_{3/2}$	0.31	0.2	$6S_{1/2}$ - $6D_{3/2}$	12.56	306	$7S_{1/2}$ - $7D_{3/2}$	8.09	119
$5S_{1/2}$ - $6D_{3/2}$	2.23	8	$6S_{1/2}$ - $7D_{3/2}$	7.91	106	$7S_{1/2}$ - $8D_{3/2}$	5.79	53
$5S_{1/2}$ - $7D_{3/2}$	2.08	6	$6S_{1/2}$ - $8D_{3/2}$	5.442	46.7	$7S_{1/2}$ - $9D_{3/2}$	4.169	26.4
$5S_{1/2}$ - $8D_{3/2}$	1.75	4	$6S_{1/2}$ - $9D_{3/2}$	4.047	24.9	$7S_{1/2}$ - $10D_{3/2}$	3.172	14.6
$5S_{1/2}$ - $9D_{3/2}$	1.47	3.0	$6S_{1/2}$ - $10D_{3/2}$	3.173	15.0	$7S_{1/2}$ - $11D_{3/2}$	2.521	9
$5S_{1/2}$ - $4D_{5/2}$	40.37	3696	$6S_{1/2}$ - $5D_{5/2}$	41.23	5111	$7S_{1/2}$ - $6D_{5/2}$	40.98	4487
$5S_{1/2}$ - $5D_{5/2}$	0.33	0.2	$6S_{1/2}$ - $6D_{5/2}$	14.76	423	$7S_{1/2}$ - $7D_{5/2}$	8.73	138
$5S_{1/2}$ - $6D_{5/2}$	2.69	11	$6S_{1/2}$ - $7D_{5/2}$	9.432	150	$7S_{1/2}$ - $8D_{5/2}$	6.516	67
$5S_{1/2}$ - $7D_{5/2}$	2.51	9	$6S_{1/2}$ - $8D_{5/2}$	6.525	67.2	$7S_{1/2}$ - $9D_{3/2}$	4.755	33.8
$5S_{1/2}$ - $8D_{5/2}$	2.12	6	$6S_{1/2}$ - $9D_{3/2}$	4.865	36.1	$7S_{1/2}$ - $10D_{5/2}$	3.641	19.2
$5S_{1/2}$ - $9D_{3/2}$	1.78	5	$6S_{1/2}$ - $10D_{5/2}$	3.819	21.7	$7S_{1/2}$ - $11D_{5/2}$	2.905	12.0
$\alpha_{q,Tail}$		224	$\alpha_{q,Tail}$		644	$\alpha_{q,Tail}$		478
$\alpha_{q,core}$		35.35	$\alpha_{q,core}$		86.38	$\alpha_{q,core}$		125.18
$\alpha_{q,vc}$		~ 0	$\alpha_{q,vc}$		~ 0	$\alpha_{q,vc}$		~ 0
Total		**6469**	**Total**		**10400**	**Total**		**8512**
Others		6520[1]	Others		10470[1]			
		6479[2]			10390[2]			
		6525[3]			10521[4]			

1. S. G. Porsev et. al., J. Chem. Phys. 119, 844 (2003).
2. J. Jiang et. et.al., Data Nucl. Data Tables 101, 158 (2015).
3. M. S. Safronova, Phys. Rev. A 83, 052508 (2011). 4. M. S. Safronova, Phys. Rev. A 94, 012505 (2016).

H. Kaur, S. Singh, B. Arora, B. K. Sahoo Phys. Rev. A 105, 032819 (2022)

H. Kaur, V. Badhan, B. Arora, B. K. Sahoo Phys. Rev. A 106, 042813 (2022)

ATOMIC THEORY: Where do we go from here?

How can we improve calculations to advance atomic quantum technologies for new physics?

How can we solve the long-standing questions of atomic theory?

Ensure easy access to the developed methods

METHODS

Challenge is to solve for the repulsion term in Hamiltonian. Perturbative and variational methods are used to handle the repulsion term but these methods are not feasible for atoms having large number of electrons

Many Body Hamiltonian

$$H(\vec{r}_1, \vec{r}_2, \cdots, \vec{r}_N) = \sum_{i=1}^{N} h_0(\vec{r}_i) + \frac{1}{2} \sum_{i \neq j}^{N} \frac{1}{|\vec{r}_{ij}|}$$

One Electron Dirac Hamiltonian

$$h_0(\vec{r}) = c\,\alpha \cdot p + \beta c^2 + V_{nuc}(\vec{r})$$

Dirac Hartree Fock method can solve for this hamiltonian with much lesser computational efforts
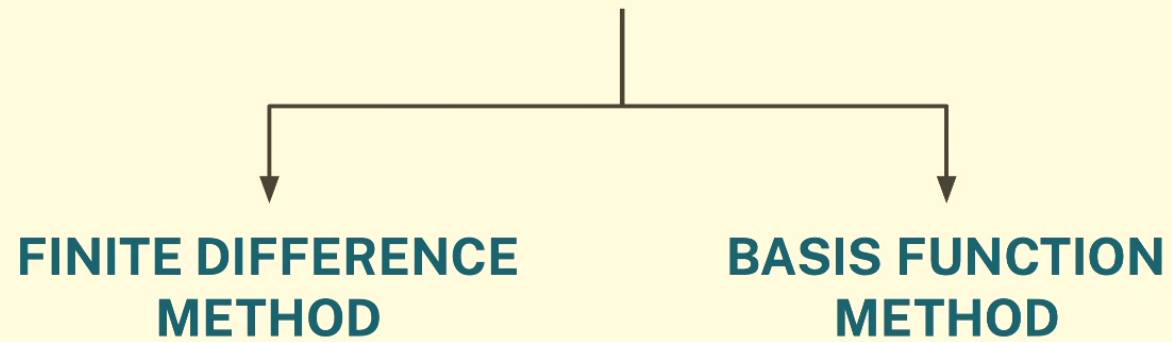
Dirac Hartree Fock

- Independent Particle Approximation
- Central Field Model
- Variational Method
- Self Consistent
- Works for Heavier Atoms

Post Hartree Fock

- Many Body Perturbation Theory
- Configuration Interaction
- Coupled Cluster

METHODS TO SOLVE DHF

FINITE DIFFERENCE METHOD

BASIS FUNCTION METHOD

FINITE DIFFERENCE METHOD

A code is made to solve N electron Hamiltonian numerically by using Adams-Moulton integration to calculate the integration of Dirac Hartree Fock differential equation

k + 1 point
Adams-Moulton integration

$$y[n+1] = y[n] + \frac{h}{D} \sum_{j=1}^{k+1} a[j]\, f[n-k+j]$$

Key Points

An initial Guess Energy is given at the start and then its is adjusted to obtain

Correct Number of Nodes
By optimizing energy values to establish accurate upper and lower bounds, ensuring the correct number of nodes.

Removing discontinuity
By removing discontinuity of wave function at classical turning point using inward integration and outward integration with an accuracy of 10^{-9}.

Correct Behaviour at zero and infinity
By defining starting point for inward and outward integration at zero and infinity to ensure the solution exhibits correct behavior from the very beginning.

TYPES OF BASIS

Slater Type Orbitals

Gaussian Type Orbitals

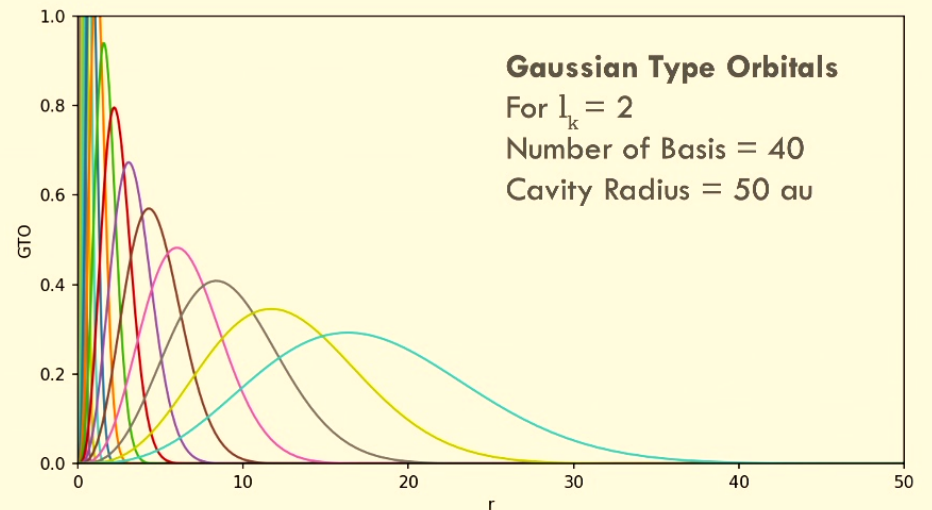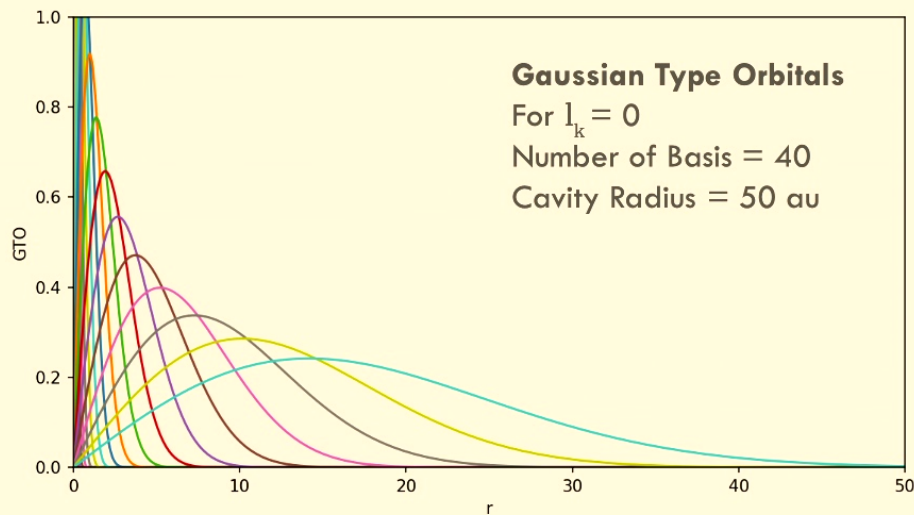**B-Splines**
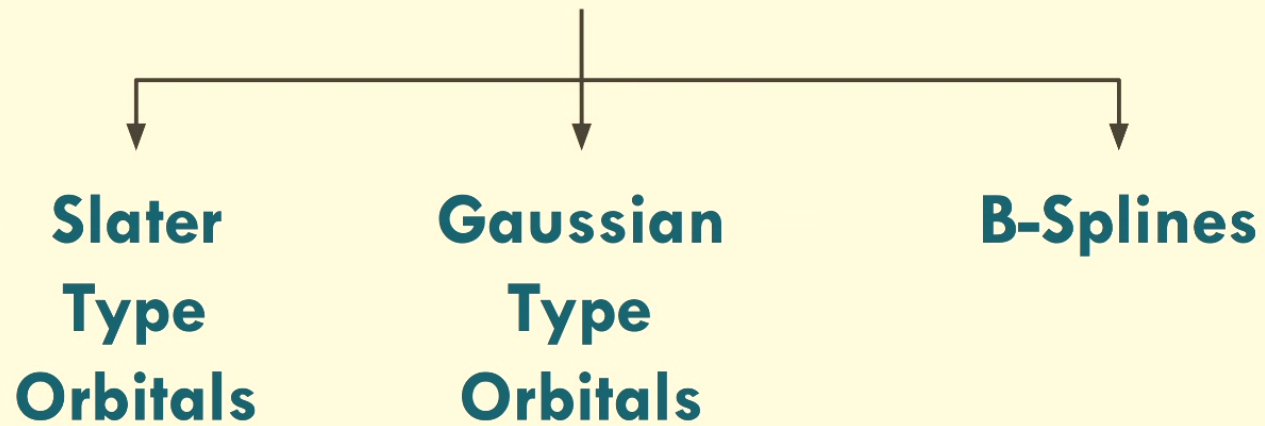
GAUSSIAN TYPE ORBITALS (GTOs)

GTOs are the most dominant basis functions used in atomic structure program packages

Gaussian Type Orbitals

$$\pi_i^{GTO}(r) \propto r^{l_\kappa} e^{-\alpha_{\kappa,i}\, r^2}$$

Key Points

- Most widely used Basis set in computational atomic and molecular calculations.
- Provides very reliable and highly accurate results for atomic properties.

Gaussian Type Orbitals
For $l_k = 0$
Number of Basis = 40
Cavity Radius = 50 au

Gaussian Type Orbitals
For $l_k = 2$
Number of Basis = 40
Cavity Radius = 50 au

B-SPLINES BASIS

B-Splines are general type of curves having control points
and each control point is associated with a basis function

The B-Spline of order k on knot sequence is defined by following relations

B-Spline Basis $\quad \pi_{i,k}(x) = \frac{x-t_i}{t_{i+k-1}-t_i}\pi_{i,k-1}(x) + \frac{t_{i+k}-x}{t_{i+k}-t_{i+1}}\pi_{i+1,k-1}(x)$

Where $\quad \pi_{i,1}(x) = \begin{cases} 1, & t_i \leq x < t_{i+1} \\ 0 \end{cases}$
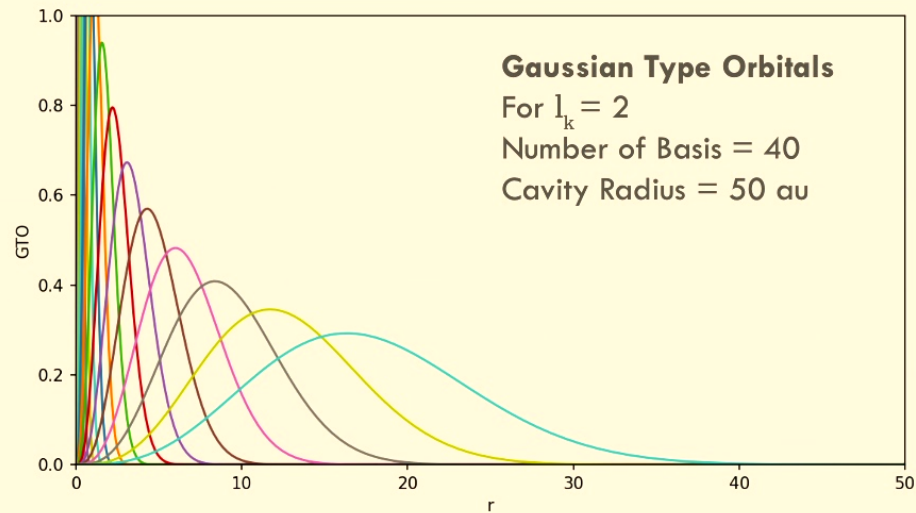
Key Points

- An important property of B-Splines is that they and their derivatives are continuous.
- B-Splines provides a high-quality basis function that can allow one to study even small relativistic effects in atoms.
- B-Splines are finite Basis sets and satisfies completeness within the cavity radius.

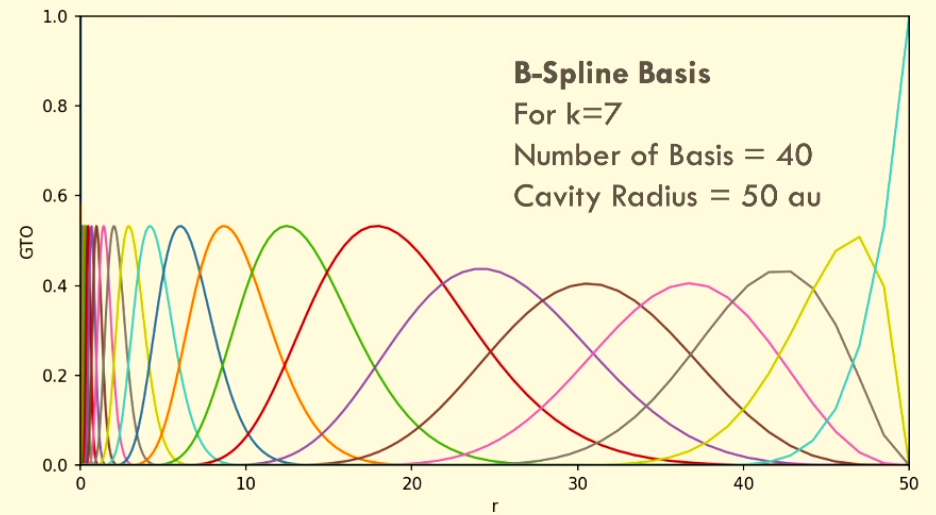B-Spline Basis
For k=7
Number of Basis = 40
Cavity Radius = 50 au
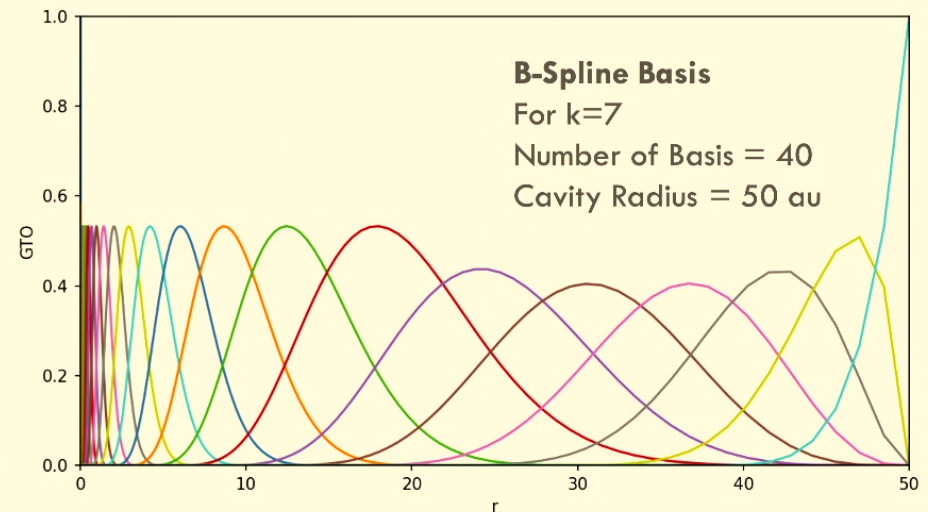
BASIS

Different bases accurately predict the behavior of the wavefunction at varying distances from the nucleus.

Gaussian Type Orbitals

Gaussian Type Orbitals
For $l_k = 2$
Number of Basis = 40
Cavity Radius = 50 au

B-Spline Basis

B-Spline Basis
For k=7
Number of Basis = 40
Cavity Radius = 50 au

BASIS WAR

There are some properties which are very sensitive to the chosen basis and the dependence of such properties on basis has not been studied in atomic physics community

The War

- Atomic structure calculations vary across research groups due to differing basis used.
- While groups often claim superiority based on basis set quality, the impact of these differences remains underexplored.
- A standardized global basis set is needed to address these inconsistencies.
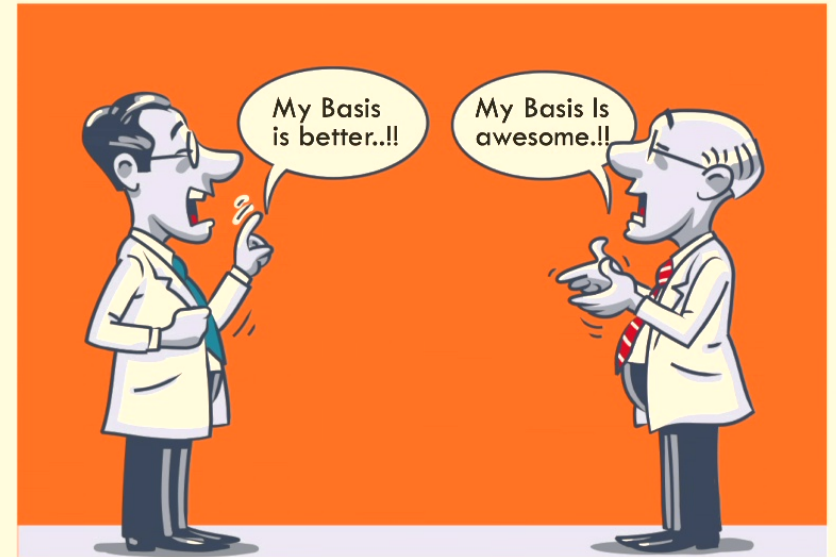
Our Role

- We study the impact of different basis sets on atomic property calculations.
- Aim to propose the best basis for various properties and post-Hartree-Fock methods.
- Develop an optimization method to reduce computational effort.

COMPARISON DIRAC-HARTREE-FOCK

Here we compare radial integral of hyperfine interaction due to electric and magnetic multipolar moments of a point like nucleus using GTOs and B-Spline with Finite Difference method

(Cs)

Electric Multipolar Moments

$$I_{EJ}(nk) = \int_0^\infty \frac{dr}{r^{J+1}}(P^2(nk) + Q^2(nk))$$

Magnetic Multipolar Moments

$$I_{MJ}(nk) = 2\int_0^\infty \frac{dr}{r^{J+1}}P(nk)Q(nk))$$

State	Basis	Energy	M1 HFI	E2 HFI	M3 HFI
$6p_{3/2}$	FD	-0.8378548[-1]	4.649102[-3]	6.693969[-1]	8.725185[0]
	GTO	-0.8378548[-1]	4.649107[-3]	6.697346[-1]	1.361816[1]
	B-Spline	-0.8378548[-1]	4.649107[-3]	6.694088[-1]	8.625503[0]
$5d_{3/2}$	FD	-0.6441960[-1]	-3.543797[-3]	1.702462[-1]	-8.950547[-1]
	GTO	-0.6441964[-1]	-3.543808[-3]	1.782267[-1]	-2.725900[1]
	B-Spline	-0.6441964[-1]	-3.543807[-3]	1.702471[-1	-5.129381[-1]

COMPARISON POST-DIRAC-HARTREE-FOCK

Cs properties calculated using 40 basis:i) B-Spline (k=9) with MIT Bag Model and ii) GTOs Even Tempered with DKB in cavity radius 110 a.u.

Electric Dipole Matrix Elements (a.u.)

n1	k1	n2	k2	B-Spline (MIT Bag)	GTOs ET (KB)	% Difference
6	-1	6	1	4.48322	4.48819	0.00111
6	-1	7	1	0.29831	0.29728	0.00345
6	-1	8	1	-0.09132	0.09035	1.98941
6	-1	9	1	-0.04247	-0.04027	0.05186
6	-1	10	1	-0.02463	0.04786	2.94274

PNC Matrix Elements ($10^{-11} i|e|a_0 (Q_W/N_n)$)

n1	k1	n2	k2	B-Spline (MIT Bag)	GTOs ET (KB)	% Difference
6	-1	6	1	0.06040	0.05852	0.03104
6	-1	7	1	0.03354	0.03296	0.01736
6	-1	8	1	-0.09132	0.02212	1.24226
6	-1	9	1	-0.01646	-0.01587	0.03541
6	-1	10	1	-0.01297	0.03508	3.70381

SPURIOUS STATES

The solution of the central field Dirac equation introduces spurious states at the start of the spectrum for k > 0, which are characterized as highly oscillating non-physical states

Arises due to

- Incomplete basis set
- Independent representation of the upper and lower component of dirac solution
- leads to incorrect behaviour in non relativistic limit

The table presents the energy values (in a.u.) of the hydrogen-like ^{133}Cs atom, where a Coulomb potential $V(r) = -Z/r$ is used in Hamiltonian. The first state associated with each relativistic quantum number κ using GTOs and B-splines (of order $k = 9$) in a cavity radius of 110 a.u and using a number of basis function 50 are presented along with the exact energies for comparison. The energies of spurious states are shown in parallel. All energy values are expressed in atomic units and the notation $x[y]$ represents $x \times 10^y$.

States	Exact	B-spline	GTOs	Spurious States	B-spline	GTOs
$1S_{1/2}$	-1.57887[+3]	-1.57887[+3]	-1.57887[+3]	$1P_{1/2}$	-1.57887[+3]	-1.57887[+3]
$2P_{1/2}$	-3.98956[+2]	-3.98956[+2]	-3.98956[+2]			
$2P_{3/2}$	-3.82011[+2]	-3.82011[+2]	-3.82011[+2]	$2D_{3/2}$	-3.82011[+2]	-3.82011[+2]
$3D_{3/2}$	-1.70362[+2]	-1.70362[+2]	-1.70362[+2]			
$3D_{5/2}$	-1.68814[+2]	-1.68814[+2]	-1.68814[+2]	$3F_{5/2}$	-1.68814[+2]	-1.68814[+2]
$4F_{5/2}$	-9.50918[+1]	-9.50918[+1]	-9.50918[+1]			
$4F_{7/2}$	-9.47704[+1]	-9.47704[+1]	-9.47704[+1]	$4G_{7/2}$	-9.47704[+1]	-9.47704[+1]
$5G_{7/2}$	-6.06960[+1]	-6.06960[+1]	-6.06960[+1]			
$5G_{9/2}$	-6.05978[+1]	-6.05978[+1]	-6.05978[+1]			

KINETICALLY BALANCED BASIS SET

Relation between upper and the lower components of the wave functions is established
to achieve correct behaviour in non relativistic limit

Kinetic Balance

Lower component of the wave functions related to
the upper component by the following relation

$$\Pi_{\kappa i}(r) = \begin{bmatrix} \pi_{\kappa i}^{P}(r) \\ 0 \end{bmatrix}, \quad i = 1, \ldots n$$

$$\Pi_{\kappa i}(r) = \begin{bmatrix} 0 \\ {}^{d}\pi_{\kappa i}^{P}(r) \end{bmatrix}, \quad i = n+1, \ldots 2n$$

where

$$|{}^{d}\pi^{P}\rangle = \frac{1}{2mc}(d/dr + \kappa/r)|\pi^{P}\rangle$$

Dual Kinetic Balance

Both upper and lower component of the wave function
are related to each other by the following relation

$$\Pi_{\kappa i}(r) = \begin{bmatrix} \pi_{\kappa i}^{P}(r) \\ {}^{d}\pi_{\kappa i}^{P}(r) \end{bmatrix}, \quad i = 1, \ldots n.$$

$$\Pi_{\kappa i}(r) = \begin{bmatrix} {}^{d}\pi_{\kappa i}^{Q}(r) \\ \pi_{\kappa i}^{Q}(r) \end{bmatrix}, \quad i = n+1, \ldots 2n,$$

where

$$|{}^{d}\pi^{P}\rangle = \frac{1}{2mc}(d/dr + \kappa/r)|\pi^{P}\rangle$$

$$|{}^{d}\pi^{Q}\rangle = \frac{1}{2mc}(d/dr - \kappa/r)|\pi^{Q}\rangle.$$

HYPERFINE CONSTANTS

A comparison of magnitudes of hyperfine constants (A_{hfs}) of ^{133}Cs atom calculated using all order methods with GTOs and B-spline basis sets is presented, highlighting the impact of no balance (NB) versus dual kinetic balance (DKB) on results. Plots of magnitude A_{hfs} against the principal quantum number (n) are provided for various total angular momentum states: (a) $nS_{1/2}$, (b) $nP_{1/2}$, (c) $nP_{3/2}$, (d) $nD_{3/2}$, and (e)$nD_{5/2}$. The vertical axes in all subplots are presented on a logarithmic scale.


(a)
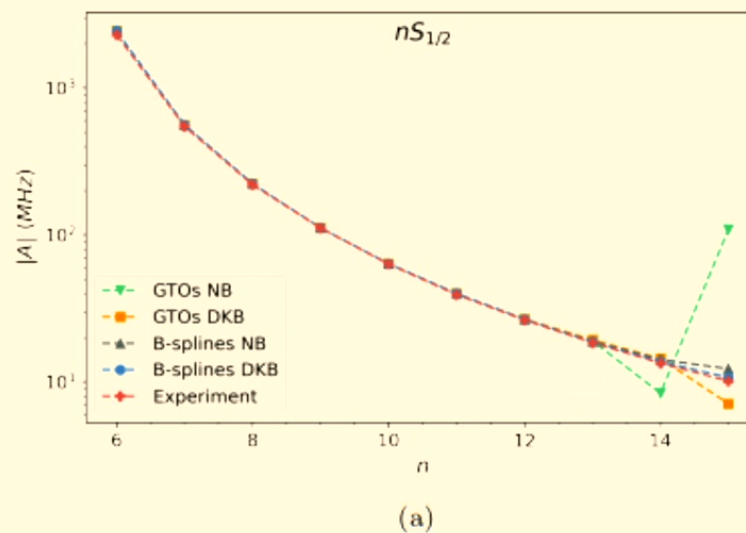
HYPERFINE CONSTANTS
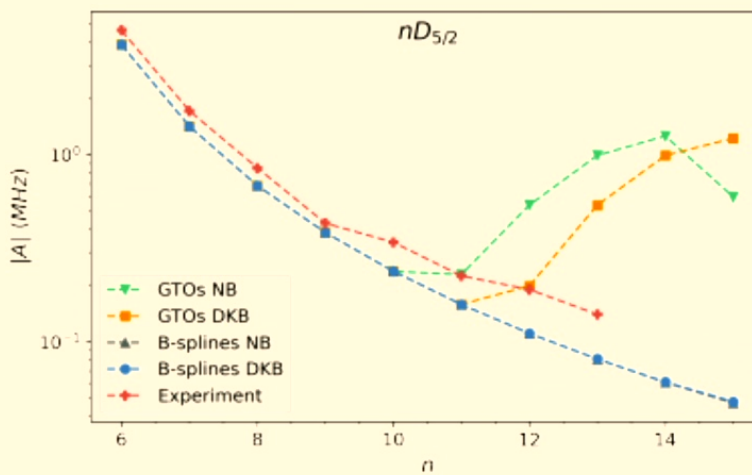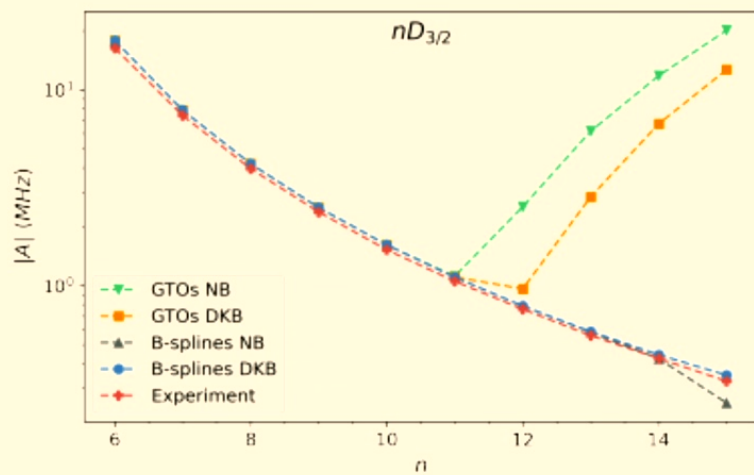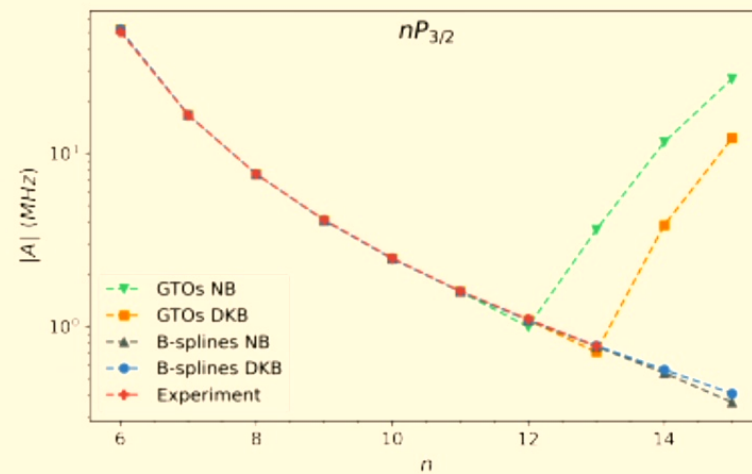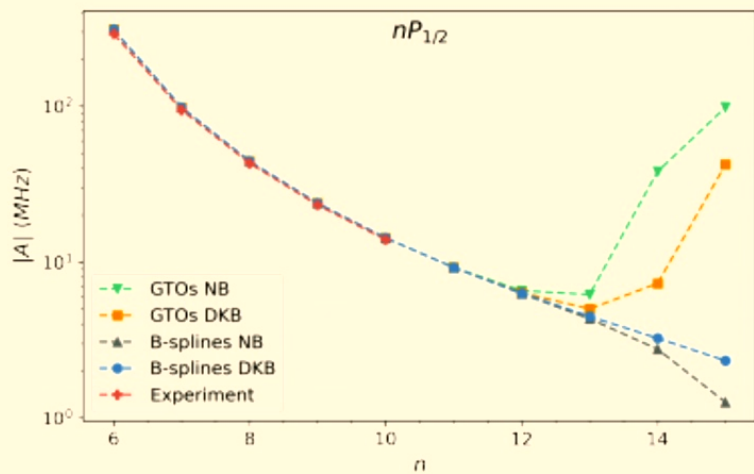
DIPOLE POLARIZABILITIES FOR 5D$_{5/2}$

The table presents the core, main and tail contribution to dipole polarizabilities of the $5d_{5/2}$ state using GTOs-DKB and B-splines-DKB basis sets. All values are expressed in atomic units and the notation $x[y]$ represents $x \times 10^y$.

$5d_{5/2}$	GTOs-DKB	B-splines-DKB
Core	1.63145[1]	1.63145[1]
Main	-6.70242[2]	-7.08532[2]
Tail	4.90417[-1]	4.46684[1]
Total	-6.53437[2]	-6.47549[2]

BREAKDOWN OF CONTRIBUTIONS FOR 5D$_{5/2}$
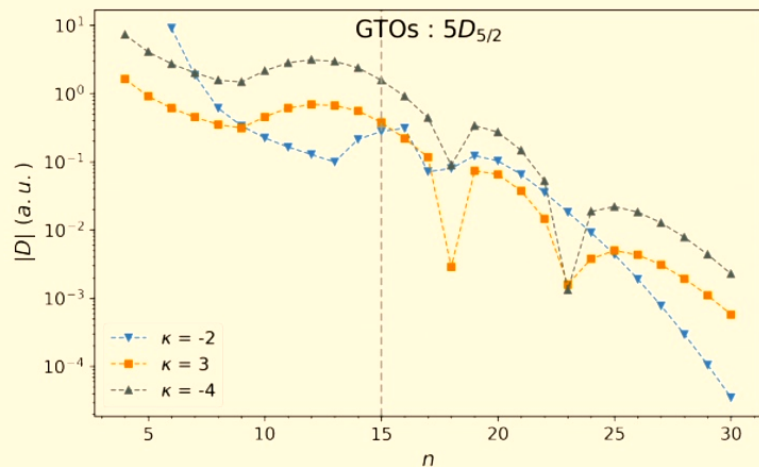
(a)
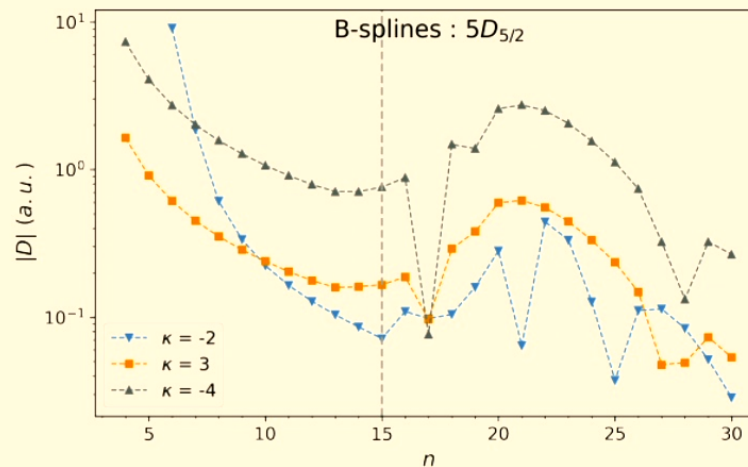
(b)

The magnitude of the matrix elements corresponding to the transitions that contribute to the polarizability of $5D_{5/2}$ were computed using AO and DHF method with (a) GTOs and (b) B-splines with the dual kinetic balance (DKB). The presented magnitude of matrix elements pertain to transitions from the $nP_{3/2}$, $nF_{5/2}$, and $nF_{7/3}$ states. In the figure, a vertical dotted line signifies the n state beyond which the matrix elements were determined using the DHF approximation. The vertical axes in all subplots are presented on a logarithmic scale.

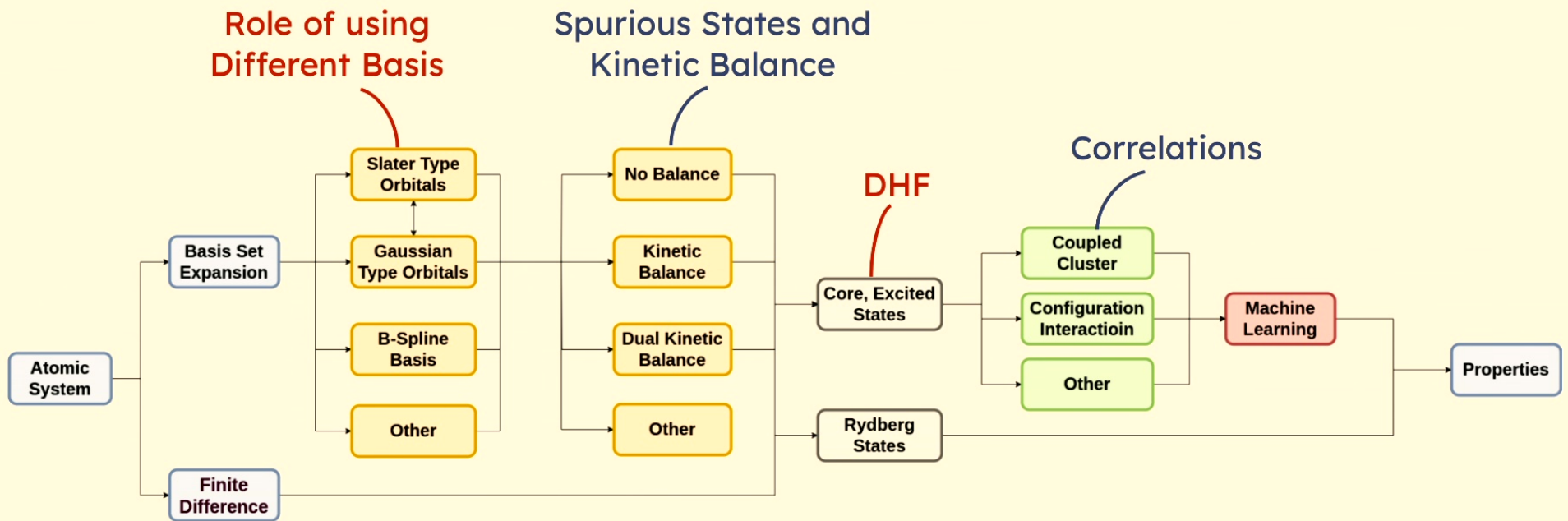# Problems with currently available atomic community codes

- Old - developed initially in 1980s and 1990s, with later updates

- Unsupported or unwieldy (too many updates by many people)

- Designed to produce large volumes of low-precision data

- Poorly documented and/or require expert knowledge to use

- No estimates of how accurate the results are

- Do not serve the needs of the present community

- There are very few groups in the world developing new atomic codes

APP

- Open access, readily usable to the atomic physics community and their fields of application

- Cloud based (no installation required)

- Requiring minimum knowledge of coding - supplying only a few parameters that describe their request

- Will benefit non-research organisations/start-ups

- Will explore new ways of combining experimental data and computation for better results

- Provide a wide variety of data, where the methodology is already developed.

- Develop novel algorithms and optimization techniques that enable atomic physics applications to scale in terms of time and problem size

WORKFLOW